

REINFORCED-SOIL EMBANKMENT ON SOFT FOUNDATION

05
14672

Tien H. Wu

The Ohio State University, 2070 Neil Ave., Columbus, OH, 43210

January, 2000

Sponsoring Agencies: Ohio Department of Transportation and U.S. Department of Transportation, Federal Highway Administration.

This report was prepared in cooperation with the Ohio Dept. of Transportation and the U.S. Dept. of Transportation, Federal Highway Administration. The contents of the report reflect the views of the author, who is responsible for the facts and the accuracy of the data presented herein. The contents do not necessarily reflect the official views or policies of the Ohio Department of Transportation or the Federal Highway Administration. This report does not constitute a specification or regulation.

TE
210.8
.03
W8
2000x



EXECUTIVE SUMMARY: REINFORCED-SOIL EMBANKMENT ON SOFT FOUNDATION

Principal Investigator: Tien H. Wu, The Ohio State University
State Job No. 14672(0)

FHWA/OH-2000/002
FOR COPIES OF THIS REPORT, CONTACT:
Ohio Department of Transportation
Mr. Roger L. Green
(614) 275-1381
rogreen@dot.state.oh.us

A section of I-670 in Columbus, OH, constructed during 1997-1998, includes a 33 ft.(10m) high embankment over a deposit of very soft sludge. The design used geosynthetics for reinforcement of the embankment and wick drains to accelerate the consolidation in the sludge. Stage construction was used to allow consolidation of the sludge. To verify the design assumptions, a test embankment was completed in 1993. The performance of the test embankment provided the information for the design of the full-scale embankment. This project provided the opportunity to demonstrate the application of research findings from the test embankment to actual design and construction.

The objective was to demonstrate how research findings can be used in design and construction. This report shows (1) how the results of the test embankment were used in the design of the full-scale embankment and prediction of the embankment performance, (2) how observation of the embankment performance can be used as construction control and (3) how the results can be used in future application of similar technology.

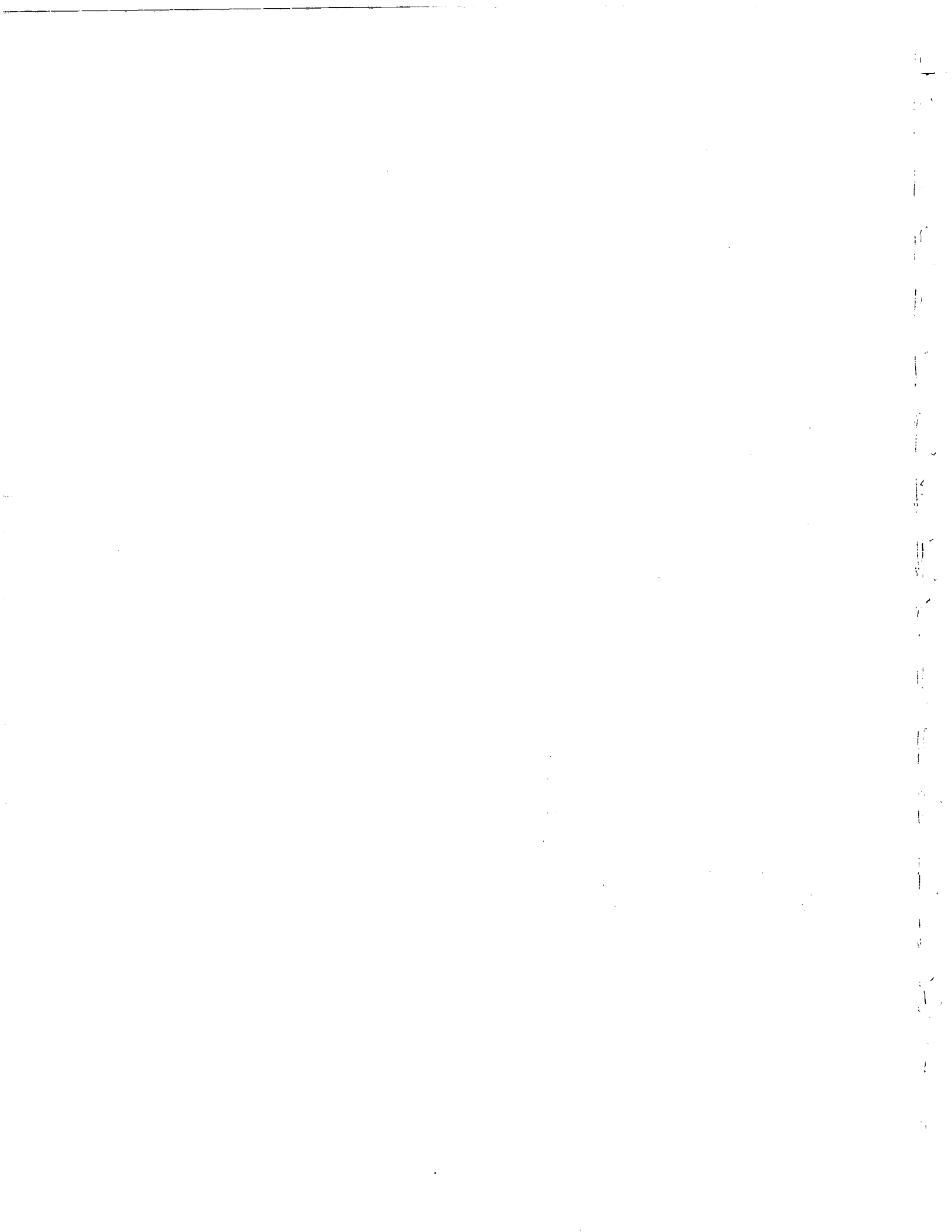
In this study, predictions of consolidation rate, settlement, horizontal movement, geotextile strain and sludge strength were made using conventional and finite-element methods and material properties determined from laboratory tests and performance of the test embankment. Overall, the prediction methods used here can estimate the right order of magnitude of consolidation rate, displacement, strain, and strength to an accuracy of 50 % or better.

Our recommendation is that the procedures used in the measurement of material properties, the design of the embankment, the prediction of embankment performance and the use measurements during construction for construction control provide an effective methodology that can be applied to the design and construction of other reinforced-soil embankments over soft ground.

The results of this project can be implemented through the use of the procedures developed here for the design and construction of future projects. The general approach of using a test embankment to verify critical design assumptions and careful monitoring of performance during construction as a part of construction control has proven to be successful. More specifically, the laboratory tests, the methods for estimating rate of consolidation, strength after consolidation, and stability, and the program for monitoring embankment performance for construction control can be implemented in future projects involving embankments on soft ground. This report and the related reports can serve as reference material for future projects.



1. Report No. FHWA/OH-2000/002	2. Government Accession No.	3. Recipient's Catalog No. 3 1980 00019 3710	
4. Title and Subtitle REINFORCED-SOIL EMBANKMENT ON SOFT FOUNDATION		5. Report Date January, 2000	
		6. Performing Organization Code	
7. Author(s) T. H. Wu		8. Performing Organization Report No.	
		10. Work Unit No. (TRAIS)	
9. Performing Organization Name and Address The Ohio State University Department of Civil Engineering Columbus, OH 43210		11. Contract or Grant No. State Job No. 14672(0)	
		13. Type of Report and Period Covered Final Report	
12. Sponsoring Agency Name and Address Ohio Department of Transportation 1600 West Broad Street Columbus, OH 43223		14. Sponsoring Agency Code	
		15. Supplementary Notes Prepared in cooperation with the U.S. Department of Transportation, Federal Highway Administration	
16. Abstract <p>A section of I-670 contains an embankment over a deposit of soft sludge. The design used geotextiles for soil reinforcement and wick drains to accelerate the consolidation in the sludge. Stage construction was used to allow consolidation of the sludge. To verify the design assumptions, a test embankment was built in 1993 and the observed performance of the test embankment provided the necessary verification. The objective of this project was to demonstrate how the findings from the test embankment was used in design and construction.</p> <p>Predictions of consolidation rate, settlement, horizontal movement, geotextile strain and sludge strength were made using conventional and finite element methods and material properties determined from laboratory tests and performance of the test embankment. Overall, the prediction methods estimated the right order of magnitude of consolidation rate, settlement, horizontal movement, geotextile strain and sludge strength.</p> <p>Our conclusion is that the procedures used in the measurement of material properties, embankment design, prediction of embankment performance, and monitoring of embankment performance during construction for construction control provide an effective methodology that can be applied to future design and construction of embankments over soft ground. The results of this study can be implemented through the use of the procedures developed here in future projects</p>			
17. Key Words consolidation, embankment on soft ground, geotextiles, slope stability, wick drains.		18. Distribution Statement No Restrictions. This document is available to the public through the National Technical Information Service, Springfield, Virginia 22161	
19. Security Classif. (of this report) Unclassified	20. Security Classif. (of this page) Unclassified	21. No. of Pages	22. Price



REINFORCED-SOIL EMBANKMENT ON SOFT FOUNDATION

Tien H. Wu

The Ohio State University, 2070 Neil Ave., Columbus, OH, 43210

January, 2000

Sponsoring Agencies: Ohio Department of Transportation and U.S. Department of Transportation, Federal Highway Administration.

This report was prepared in cooperation with the Ohio Dept. of Transportation and the U.S. Dept. of Transportation, Federal Highway Administration. The contents of the report reflect the views of the author, who is responsible for the facts and the accuracy of the data presented herein. The contents do not necessarily reflect the official views or policies of the Ohio Department of Transportation or the Federal Highway Administration. This report does not constitute a standard, specification or regulation.

CONTENTS

1. INTRODUCTION	1
2. OBJECTIVES	1
3. DESCRIPTION OF RESEARCH	2
3.1 Design Considerations.	2
3.2. Observations of Performance	3
3.3. Prediction of Performance	9
4. RESULTS	10
4.1. Radial Consolidation	10
4.2. Finite Element Method.	15
4.3. Settlement	16
4.4. Horizontal Displacement	26
4.4. Reinforcement Strain	27
4.5. One-dimensional Compression	29
4.6. Undrained Shear Strength	30
5. CONCLUSIONS AND RECOMMENDATIONS	35
6. IMPLEMENTATION	36
APPENDIX A. MEASURED SETTLEMENT, POREPRESSURE, HORIZONTAL DISPLACEMENT AND GEOTEXTILE STRAIN	37
APPENDIX B. SOLUTION FOR TIME-DEPENDENT LOADING	38
APPENDIX C. UPDATING WITH OBSERVED PERFORMANCE	39
APPENDIX D. REFERENCES	40

LIST OF TABLES

3.1. List of Measurements	8
4.1 Calculated and Measured Consolidation	12
4.2. Results of Laboratory Consolidation Tests	14
4.3 Updated Material Properties	15
4.4. Updated Preconsolidation Pressures (σ_p')	16
4.5. Calculated and Measured Vertical Displacements	26
4.6 Calculated and Measured Horizontal Displacements	27
4.7 Measured and Calculated Reinforcement Strains	28
4.8 Calculated and Measured Shear Strengths	33

LIST OF FIGURES

3.1. Plan of Project	4
3.2. Cross Sections, Sta. 392 and 395	5
3.3. Cross Sections, Sta. 397 and 401	6
3.3. Cross Sections, Sta. 406 and 409	7
4.1a. FEM Mesh, Sta. 397	18
4.1b. Vertical Displacements Computed by FEM, Sta. 397	19
4.1c. Horizontal Displacements Computed by FEM, Sta. 397	20
4.1d. Reinforcement Strain Computed by FEM, Sta. 397	21
4.2a FEM Mesh, Sta. 395	22
4.2b. Vertical Displacements Computed by FEM, Sta. 395	23
4.2c. Horizontal Displacements Computed by FEM, Sta. 395	24
4.2d. Reinforcement Strain Computed by FEM, Sta. 395	25
4.3a. Stress State for Vane Shear Test	32
4.3b. Mohr's Circle of Stress for Vane Shear Test	32
4.4. Measured Vane Shear Strengths	34
B.1. Solution for Radial Drainage under Time-dependent Loading	38

Acknowledgements: The author wishes to thank the following individuals for their contributions to this study. E. C. Geiger, R. Mayo, and R. Morris provided many necessary details about the construction of the embankment, and M. R. Stouffer provided the results of inclinometer measurements. All are with Ohio Dept. of Transportation. Measurements of settlement and porepressure were made by S. M. Gale of Gale-Tec Engineering and made available to the writer by Clyde E. Williams and Assoc. S. X. Zhou made the finite element analysis.

1. INTRODUCTION

A section of I-670 in Columbus, OH, constructed during 1997-1998, includes a 33 ft.(10m) high embankment over a deposit of very soft sludge. Because the sludge is too soft to support the embankment, the embankment design requires the use of geosynthetics for reinforcement of the embankment and wick drains to accelerate the consolidation in the sludge. To verify the design assumptions, a test embankment was completed in 1993. Its performance was measured with an extensive set of instrumentation. The results were evaluated by the designer (STS Consultants, 1993), Ohio Dept. of Transportation, and Ohio State Univ.(Wu, 1996). The performance of the test embankment generally support the assumptions used in design.

The construction plan for the I-670 embankment included extensive instrumentation which provided data used for construction control. Stage construction was used to allow consolidation of the sludge. This project provided an unusual opportunity to demonstrate the application of research findings from the test embankment to actual design and construction. In view of the fact that the successful use of geosynthetics in an embankment and consolidation of a very soft sludge represent an unusual application of new technology, the proper documentation of this experience is considered worthwhile in order to promote the use of the new technology.

Construction of the embankment started in July of 1997 and was completed at the end of 1998. The measured performance of the embankment was evaluated with current methods for analysis and design and summarized in this report.

This study is closely related to the construction project and the measurements made to monitor embankment performance. The location of the measurements and embankment cross-sections are identified with references to the construction plans of Ohio Dept. of Transportation (ODOT) (State of Ohio, 1996). To present the results in a form that is readily useable by ODOT engineers and to avoid undue conversions, we have retained the English units used for station numbers and elevations on the construction plans and for the data from the measurements. Both English and SI units are given for material properties that are of general interest.

2.OBJECTIVES

The objective is to demonstrate how a new technology and research findings can be used in design and construction. The experience gained from this project should encourage future use of the technology. Specifically, we wish to show (1) how the results of the test embankment were used in the design of the full-scale embankment and prediction of the embankment performance, (2) how observation of the embankment performance can be used as construction control and (3) how the predicted and observed performances can be used as experience in future application of similar technology.

3. DESCRIPTION OF RESEARCH

3.1 Design Considerations.

As background information, we review first the evaluation of embankment stability. Stability analyses using strengths measured during site exploration (STS Consultants, 1987) and in laboratory experiments (Wu, 1996) gave the following results. For the first stage of the test embankment with a height of 10 ft. (3m), the calculated safety factor is 1.3 for the undrained shear strength and 3.3 for the drained shear strength. If the sludge is allowed to consolidate and the second stage is built to a height of 20 ft. (6m) in the undrained condition, the calculated safety factor is 2.5 (Wu, 1996). These numbers show that the embankment will be stable provided that consolidation is allowed after each stage of loading.

The two major questions during the preliminary design were: (1) will the sludge gain strength after consolidation as indicated in the laboratory tests, and (2) will the rate of consolidation be fast enough so that stage construction is feasible? The test embankment gave positive answers to both questions. To assure that both conditions are satisfied during the construction of the full-scale embankment, the final design contains specific requirements for the rate of pore pressure dissipation. The requirements are established on the following basis (STS, 1994).

The undrained shear strength at any time during construction is expressed as

$$s_u = c + U \sigma_z \tan \phi \quad [3.1]$$

where c , ϕ = shear strength parameters in total stresses, determined by consolidated-undrained triaxial tests, σ_z = vertical stress, U = degree of consolidation. The stability is estimated by the bearing capacity equation

$$q_f = s_u N_c \quad [3.2]$$

where q_f = bearing capacity, N_c = dimensionless bearing capacity number. The safety factor is

$$F_s = q_f / \gamma (h_0 + h_1) \quad [3.3]$$

where γ = unit weight of embankment material, h_0 , h_1 = existing height of embankment and height added, respectively. Adopting conservative values of $c = 0$ and $\phi = 27.5^\circ$ gives $F_s = 1.8$ for $U = 0.6$. Therefore a degree of consolidation of 0.6 under a given load increment is required before the addition of another load increment if a safety factor of 1.8 is to be maintained. This requirement was used to control the rate of construction of the embankment.

3.2. Observations of Performance

Fig. 3.1 is a plan of the project and representative cross-sections are shown in Fig. 3.2 to 3.5. It should be noted that the bottom of the sludge deposit as shown was estimated from earlier boring logs, penetration tests, and wick drain penetrations. These bottoms differ from those shown in the construction drawings (State of Ohio, 1996) which are based on ODOT's limited number of soundings and are in error by substantial amounts at several locations as shown in Fig. 3.4.

Measurements made during construction include settlement, horizontal displacement, porepressure, reinforcement strain, and shear strength. The measurements were made by Gale-Tec Engineering (Gale, 1998). Table 3.1 lists all the measurements and their locations. Details are reported separately in Gale (1999) and are not repeated here. Measured performance that is used for verification of the prediction methods are summarized in Section 4 and representative data are reproduced in Appendix A.

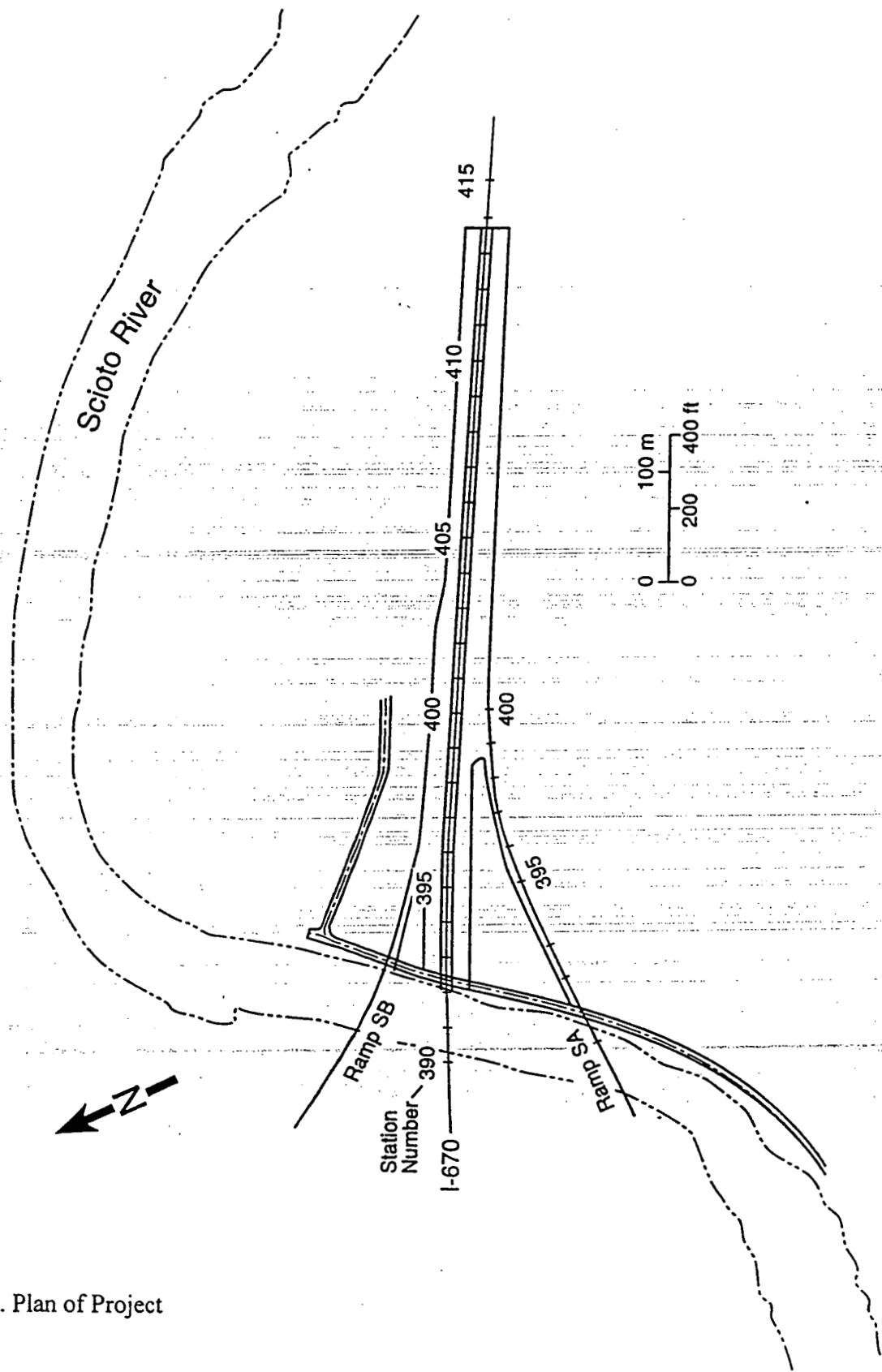
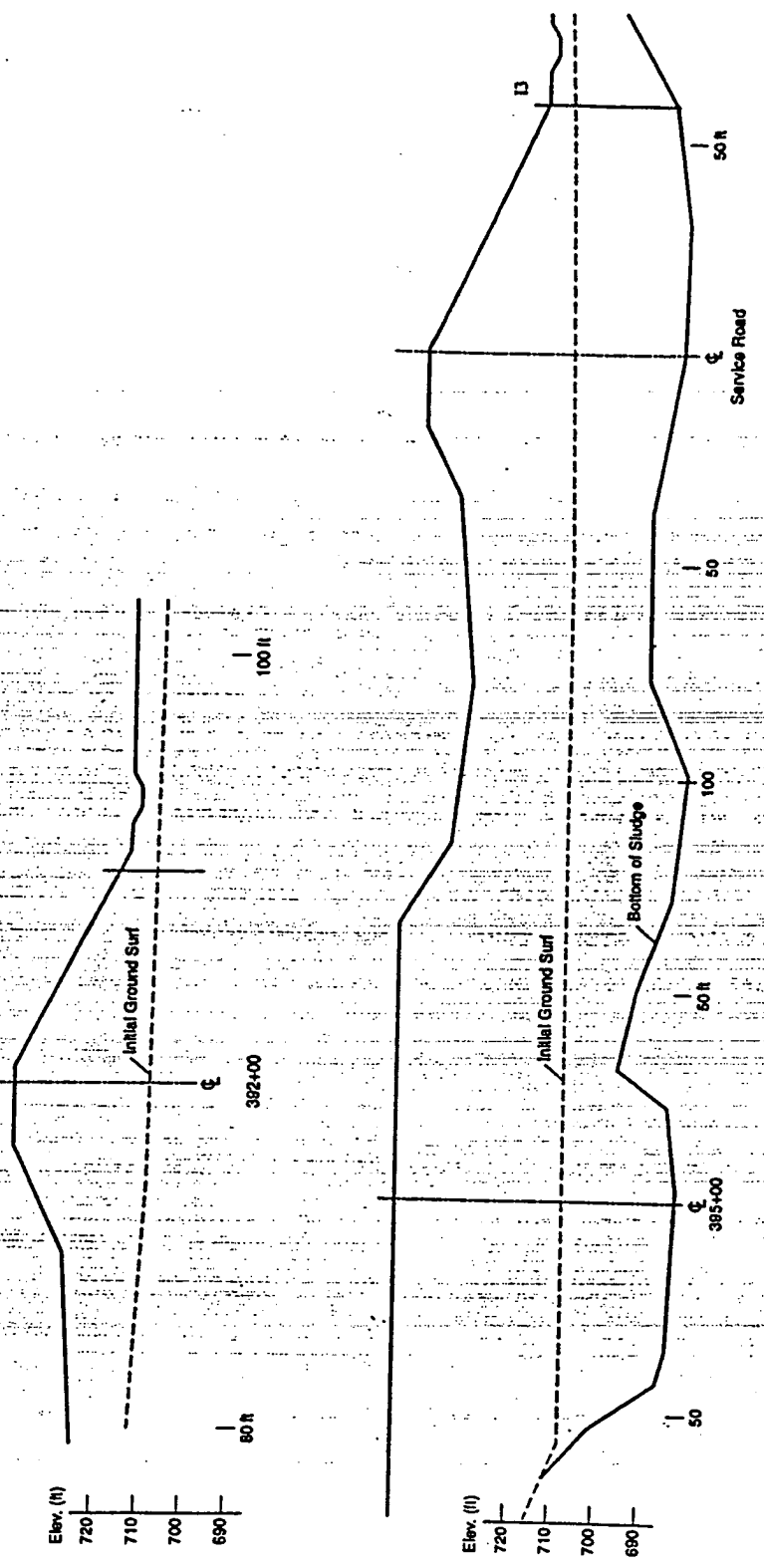


Fig. 3.1. Plan of Project



Sheet No.

Fig. 3.2. Cross Sections, Sta. 392 and 395

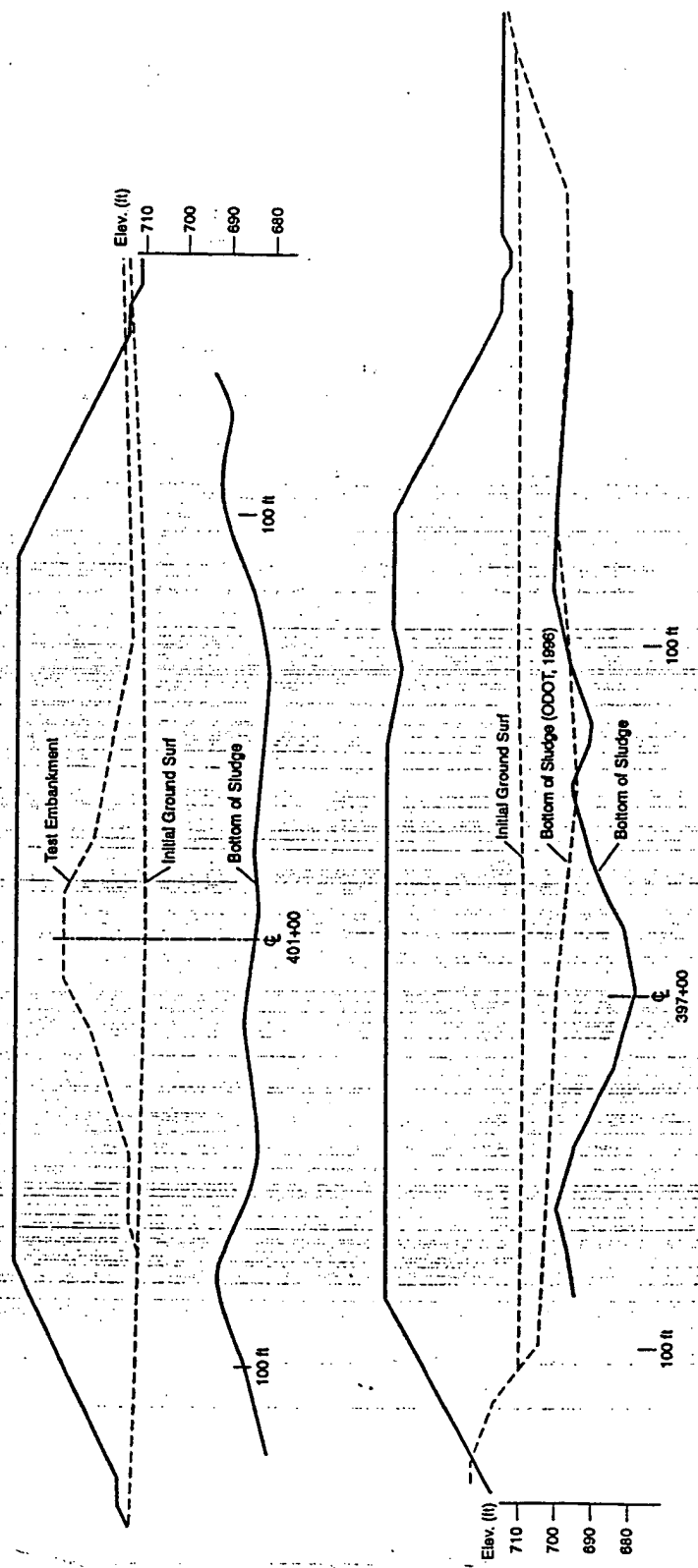


Fig. 3.3. Cross Sections, Sta. 397 and 401

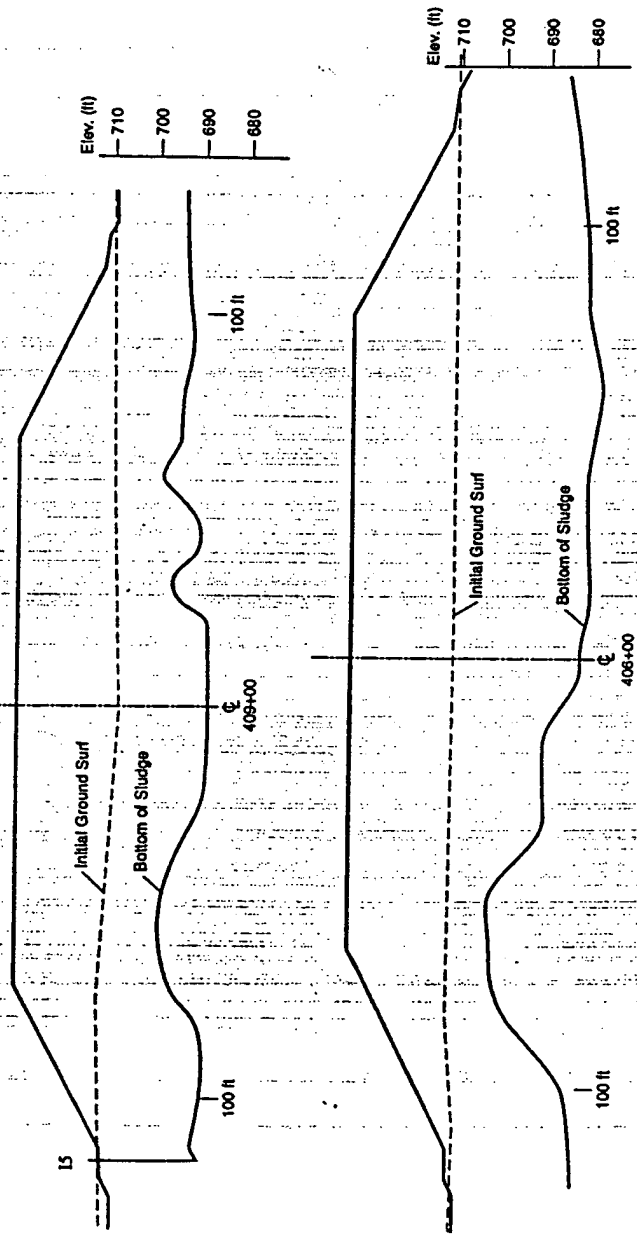


Fig. 3.4. Cross Sections, Sta. 406 and 409

Table 3.1. List of Measurements.

Station	Vertical settlement	Horizontal movement	Pore pressure		Reinforcement strain	Vane shear
	(location) ¹		(location)	(location)		
392	20 rt (SA)	50 rt	20 rt (SA)	699	rt	20 rt, cl (SA)
394 + 80						
395	cl, 20 rt (SA)	65 rt	20 rt (SA)	690, 700		cl, 20 rt (SA)
397	20 rt (SA)					
398	cl					
399	100 lt					
400	cl, 100 lt		cl, 100 lt	693, 701, 705	lt	cl, 100 lt
400 + 15						
401	cl		100 rt	703		cl
402	cl		cl	695		cl
403	cl, 90 lt		90 lt	702	rt	
403 + 85						
404	cl		cl	697 ² , 705 ²		cl
405	cl, 85 lt					
406	cl, 90 rt	125 rt	90 rt	691, 701		50 rt, 90 rt
407	cl, 85 lt, 85 rt					
408	cl, 80 rt		80 rt	695		45 rt, 80 rt
409	cl., 80 lt	115 lt.	80 lt	702		cl
409+15						lt.
409 + 70	cl					

1. Location is indicated as distance in ft., cl = centerline, rt or lt = right or left of centerline; (SA) denotes ramp SA. 2. Instrument failed.

3.3. Prediction of Performance

Predictions of embankment performance were made using conventional methods and the finite element method (FEM). Predictions were made of the rate of consolidation, the soil displacements in the vertical and horizontal directions, the reinforcement strain, and the shear strength after consolidation. This section provides an overview of the prediction methods used. To provide continuity in the presentation of the calculations and the interpretation of the results, the details about the calculations are presented in Section 4, where the calculated results are also compared with the measured performance.

The rate of consolidation is primarily controlled by the well spacing, drain dimensions, and coefficient of consolidation. The measured excess porepressure at the end of a loading period was taken as the initial porepressure. The solutions for radial consolidation by Barron (1947) and Schiffman (1958) were used to calculate the coefficient of consolidation that would give the porepressure measured at a given time after the end of the loading period. The calculated coefficients of consolidation were compared with those measured in laboratory consolidation tests (Wu, 1996). Agreement between the two sets of coefficient of consolidation should indicate that the results of laboratory consolidation tests and the theory of consolidation can provide a good estimate of the rate of consolidation in the sludge deposit.

Calculation of soil displacements and reinforcement strain in soil structures with complex geometry can be readily made with the finite element method (FEM). Commercial software are available and we used the ABAQUS (1990) because of its flexibility and because it contains bar elements and drain elements that simulate the reinforcements and drains, respectively. Calculation of the vertical displacement, or settlement, was also made by the conventional method of one-dimensional compression (Terzaghi, 1943). The assumption of one-dimensional compression can be justified for points near the center of the embankment because of the large width of the embankment. The calculated soil displacements and reinforcement strains were compared with the measured values. Agreement between calculated and measured values is taken as verification of the material properties and methods used for prediction.

Prediction of the shear strength of the sludge after consolidation was made by total stresses or by effective stresses, using the properties of the sludge determined in laboratory triaxial tests (Wu, 1996). The prediction was based on Mohr-Coulomb theory of shear strength and the stress relations as defined by Mohr's circle. The predicted strengths were compared with the strengths measured before and during construction. Agreement between calculated and measured values is taken as verification of the use of triaxial tests to predict the gain in shear strength of the sludge

4. RESULTS

4.1. Radial Consolidation

Consider the case of radial flow towards the well. The porepressure at time t and distance r from the well is (Barron, 1948)

$$u_r = \frac{4\bar{u}}{F(n)d_e^2} [r_e^2 \ln(r/r_w) - (r^2 - r_w^2)/2] \quad [4.1a]$$

$$\bar{u} = u_0 e^\lambda, \quad \lambda = -8 T_h / F(n), \quad n = r_e / r_w \quad [4.1b]$$

$$F(n) = \frac{n^2}{n^2 - 1} \ln(n) - \frac{3n^2 - 1}{4n^2} \quad [4.1c]$$

$$T_h = c_h t / r_e^2 \quad [4.1d]$$

where r_w = equivalent radius of drain = 1 in. (2.5 cm), r_e = one-half of well spacing = 3.5 ft (1m), t = time, T_h = dimensionless time for flow in the horizontal direction, \bar{u} = average porepressure, u_0 = porepressure at $t = 0$.

Installation of the drains introduces disturbance in the adjacent soil. The disturbed zone is called the smear zone. If the soil is stratified, the disturbance would reduce the permeability in the smear zone from the initial permeability k_h to k_s . The radius of the smear zone r_s is generally unknown, but experience suggest that $r_s = 2 r_m$, where r_m = equivalent radius of the mandrel = 2 in (5cm). Various studies have shown that the ratio $s = r_s / r_w$ falls within the range of 2-4 for wick drains (Hansbo, 1987; Bergado et al, 1991). Richart (1957) has shown that the effect of smear ($s > 1$) can be treated as a case of no smear ($S=1$) with a larger equivalent value of n . For s between 2 and 4, and $m = k_h / k_s = 2$, the equivalent n is between 30 and 70.

Schiffman (1958) gives solutions for \bar{u} under a uniform rate of loading. At the end of the loading period $t = t_0$, the average excess porepressure is

$$\bar{u}(T_0) = \frac{F(n)u_0}{8T_0} \{1 - e^\lambda\} \quad [4.2a]$$

where T_0 = dimensionless time for t_0 , u_0 = excess porepressure that corresponds to the applied load increment. At time t after the completion of the loading, the average excess porepressure is

$$\bar{u}(T_h) = \frac{F(n)u_0}{8T_0} \{1 - e^{-[8/F(n)]T_0}\} \{e^{-[8/F(n)](T_h - T_0)}\} \quad [4.2b]$$

Eq. [4.1a] may be used to find the porepressure midway between wells ($r = r_e$) from \bar{u} . For the given dimensions of r_w and r_e , Eq. [4.1a] becomes

$$u(r_e) \approx 1.1 \bar{u} \quad [4.3]$$

We note that this corresponds to the porepressure measured by the piezometers, which are located midway between the drains.

The load history at Sta 395 are used here to check the porepressure at the end of a loading increment ($t = t_0$). The shortest loading time is $t_0 = 5$ days for Sta. 395 from 18 to 23 Sept. 97. For $t_0 = 5$ days and $c_h = .06$ in²/min (0.39 cm²/min), Schiffman's Eq. [4.2a] was used to obtain $\bar{u} = 0.91 u_0$, which means that there was very little dissipation of porepressure during the loading period. Eq. [4.3] was used to find $u(r_e)$ from \bar{u} , given that $u(r_e) =$ measured excess porepressure. For measured $\bar{u}(r_e) = 287$ and 250 psf (13.8 and 12.0 kPa) in Cells 1 and 2, respectively, $u_0 = 315$ and 275 psf (15.1 and 13.2 kPa). The applied pressure increment, $\Delta\sigma$, is 287 psf. (13.8 kPa). This means $u_0/\Delta\sigma \approx 1$, which is what should be expected for a large loaded area that approximates one-dimensional compression. The above results provide a preliminary check on the consistency in the measured porepressures in terms of what is generally accepted modes of consolidation.

The best records of measured porepressure for comparison with predictions are those with periods during which the load remained nearly constant for complete dissipation of excess porepressure. The chosen periods are listed in Table 4.1. The measured excess porepressure at approximately $U=0.5$, was used to obtain e^λ from Schiffman's Fig. 21*, assuming $n = 70$. Then λ and the time $t_{0.5}$ at $U=0.5$ were used in Eq [4.2] and [4.1d] to calculate c_h . The calculated values of c_h are given in Table 4.1. These represent the values that would give the rate of consolidation as reflected by the measured porepressures. The range in c_h is between 0.04 and 0.6 in²/min.(0.26-3.9 cm²/min).

*For the user's convenience, this figure is reproduced in Appendix B

Table 4.1 Calculated and Measured Consolidation

Station	Location	Elev. (ft)	Period (day.mo.yr)	c_v from measured U	
				(in ² /min)	(cm ² /min)
392	20 rt (SA)	699	25,9,97-03,10,97	0.15	0.9
395	20 rt (SA)	690	23,9, 97-28,10,97	0.05	0.3
		690	5,12,97-16,3,98	0.06	0.4
		700	23,9, 97-28,10,97	0.05	0.3
		700	5,12,97-16,3,98	0.04	0.3
400	cl	693	8,12,97-2,4, 98	0.08	0.5
		701		erratic readings	
401	100 rt	703		poor response	
403	90 lt	702	17,11,97-22,4,98	0.01	0.06
406	90 rt	691	17,11,97-31,3,98	0.04	0.4
		701		0.04	0.2
408	80 rt	695	12,11,97-31,3,98	0.01	0.1
409	80 lt	702	07,11,97-27,3,98	0.05	0.2

The c_h computed from the measured porepressure is compared with the average and range of c_h obtained in the laboratory consolidation tests (Wu, 1994), which are given in Table 4.2. The coefficients of consolidation c_v and c_h are known to vary with the applied pressure, σ' . Therefore, the range between σ' from 1160-4550 psf (55.7-218 kPa) is shown in Table 4.2. However, this range is small when compared with the range between different samples, which reflect the variability of the sludge. The values in Table 4.2 give a range in c_h of 0.01-1.0 in²/min (0.06-6.5 cm²/min). The values of c_h calculated from measured porepressure fall within this range. We consider this to be sufficient indication that the consolidation theory and the laboratory results give a satisfactory prediction.

We note that n depends on the ratios m and s , neither of which are accurately known. The sensitivity of the calculated c_h to m and s can be evaluated by calculating c_h with $n = 15$ for the case of no smear, or $s = 1$. For Sta. 395, 20 ft. rt., this reduces c_h to about 0.55 of the values calculated with $n = 70$. We note that this difference is small when compared to the range of measured in the laboratory tests. This means that the c_h computed from measured porepressures is not sensitive to s and n . Hence the results are not sufficient for drawing any inferences on what may be s and n in-situ.

Table 4.2. Results of Laboratory Consolidation Tests

No.	Elev. ft (m)	e_0	C_c	C_u	c_v in ² /min (cm ² /min)	c_v in ² /min (cm ² /min)
1	712.5 (217.1)	5.1	1.9		0.011-0.025 (0.07-0.15)	
3	711.5 (216.8)	5.7	5.3		0.013-0.039 (0.08-0.25)	
7	713.5 (217.4)	5.6	3.3	0.02		0.078-0.19 (0.5-1.2)
8	713.5 (217.4)	5.6	2.2	0.06		0.16-0.052 (1.0-0.3)
9	710.5 (216.5)	5.5	2.5	0.03		0.27-0.65 (1.7-4.2)
10	710.5 (216.5)	5.5	2.8	0.04		1.3-1.1 (7.7-7.0)
11	705 (214.9)	5.8	3.4	0.04		0.013-0.008 (1.1-.05)
12	705 (214.9)	5.5	2.9	0.67		0.68-0.98 (5.5-6.3)
13	702.5 (214.1)	4.0	2.1	0.06		0.24-0.21 (1.5-1.4)
14	694.5 (211.6)	4.0	2.4	0.05		0.41-0.27 (2.6-1.6)
15	694 (211.5)	6.9	3.4	0.07		0.82-0.62 (5.2-3.6)
16	694 (211.5)	6.9	4.0	0.07		0.78-0.45 (34-2.9)
17	699 (213.0)	6.1	2.3	0.06	0.025-0.029 (0.17-0.18)	
18	699 (213.0)	6.1	3.5	0.05	0.035-0.031 (0.20.19)	
19	698 (212.7)	5.9	1.2	0.03	0.038-0.039 (0.23-0.25)	
20	686.8 (209.3)	7.7	1.6	0.04		

4.2. Finite Element Method.

The material properties for the FEM analysis are those determined for the test embankment (Wu, 1996) after updating by Zhou (1995) using the performance of the test embankment. A brief summary of the updating process is given in Appendix C. The updated material properties are summarized in Tables 4.3 and 4.4. In Table 4.4, σ_p' = preconsolidation pressure, σ_o' = overburden pressure, and γ = unit weight of soil. The quantity $(\sigma_o' + 3\gamma)$ represents the overburden plus the weight of the working platform, which is 3 ft (0.9m) thick. This was used as the initial condition because all the in-situ measurements were started after the working platform was finished.

Table 4.3 Updated Material Properties

a) Sludge				
Swelling index, κ	Compression index, λ	Stress ratio at critical state, M	Initial void ratio e_o	Poisson's ratio, ν
0.021	1.35	1.78	5.78	0.3
$C_r=0.048$	$C_c=3.11$			
b) Sand				
Young's Modulus, E_r	Poisson's ratio, ν_r	Friction angle, ϕ' (deg)	Dilation angel, ψ (deg)	Stress ratio, K
629,000 psf 30100 kPa	0.3	49	25	1.0
c) Geotextiles				
High Strength		Medium Strength		
Modulus	Poisson's Ratio	Modulus	Poisson's Ratio	
60,000 lb/ft 876 kN/m	0.25	12,000 lb/ft 175 kN/m	0.25	

d) Drains: Transmmisivity = $0.0001 \text{ ft}^3/\text{min}/\text{ft} = 0.02 \text{ l}/\text{min}/\text{m}$.

Table 4.4. Updated Preconsolidation Pressures (σ_p')

Depth	Elevation		σ_p' *		σ_0'		$\sigma_0' + 3 \gamma$	
	(ft)	(m)	(psf)	(kPa)	(psf)	(kPa)	(psf)	(kPa)
0.8	708.7	216	620	29.8	32	1.5	408	19.5
3.2	706.3	215.3	609	29.2	106	5	481	23.1
6.4	703.1	214.3	554	27.4	215	10.3	590	28.3
9.7	699.8	213.3	500	24.8	326	15.6	701	33.6
13.0	696.5	212.3	472	22.6	436	20.9	812	38.9
16.3	693.2	211.3	548	24.3	548	26.3	922	44.2
19.6	689.9	210.3	658	25.0	658	31.5	1034	49.6

* Except for sta. 401

The first prediction with FEM was made in 1997 for Sta. 397. This station was chosen because of its proximity to the site of the test embankment and because the sludge thickness as shown on the construction drawings (State of Ohio, 1996) is fairly uniform. The prediction was planned as a Type A prediction (Lambe, 1973). At this time, embankment construction was in progress and the actual construction progress up to 23, Sept., 97 was used. After this date, the embankment was raised at the rate of 2 ft. every 15 days, which was the estimated construction schedule at that time. The calculated settlement and horizontal displacements and reinforcement strains are shown in Fig. 4.1. Since the real construction schedule after 23, Sept., 97 was different, only the prediction for the final state could be used for comparison.

During the installation of the drains, it became evident that the bottom of the sludge deposit was very irregular and the bottom shown on the construction drawings are in error at several locations. The revised profile of the bottom at Sta. 397 is shown in Fig. 3.4. However, at the location where the settlement was measured, 20 ft right on Ramp SA, the revised profile show approximately the same depth of sludge as the initial profile. Therefore the FEM calculations for vertical settlement at this point should still be valid.

In Dec. 97, ODOT added inclinometer measurements to the measurement system. It was then decided to make the FEM calculation for Sta. 395, where an inclinometer tube is located. To maintain the spirit of the Type A prediction, the material properties used for Sta. 397 was retained and the construction schedule was duplicated in the calculations. The calculated vertical and horizontal displacements and reinforcement strains for the revised profile of the sludge bottom at Sta. 395 are shown in Fig. 4.2.

4.3. Settlement

The calculated vertical displacements, or settlements, at Sta. 397 and 395 are also given in Tables 4.5 and 4.6. For comparison with the measured settlements, the calculated settlements for 10, 9, 97 (Fig. 4.1b) were subtracted from the computed final settlements because settlement

measurements were started around 10, 9,97, after the working platform was finished. The calculated settlements near the shoulder , 20 ft (SA), at both stations are close to the measured settlement. The calculated settlement at the centerline of Sta. 395 is larger than the measured settlement. The ratio of measured to calculated settlements is between 0.68 and 1.16.

We should note that near the centerline of Sta. 395, the bottom of the sludge also varies along the centerline, or in the direction perpendicular to the cross-section. Between Sta. 394+70 and 394+90, and at a distance of 20 ft from the centerline, are humps in the bottom profile, where the sludge thickness is only 10-16 ft. This will certainly reduce the settlement. Therefore the problem is three-dimensional. A three-dimensional FEM analysis could be made but is outside the scope of this study.

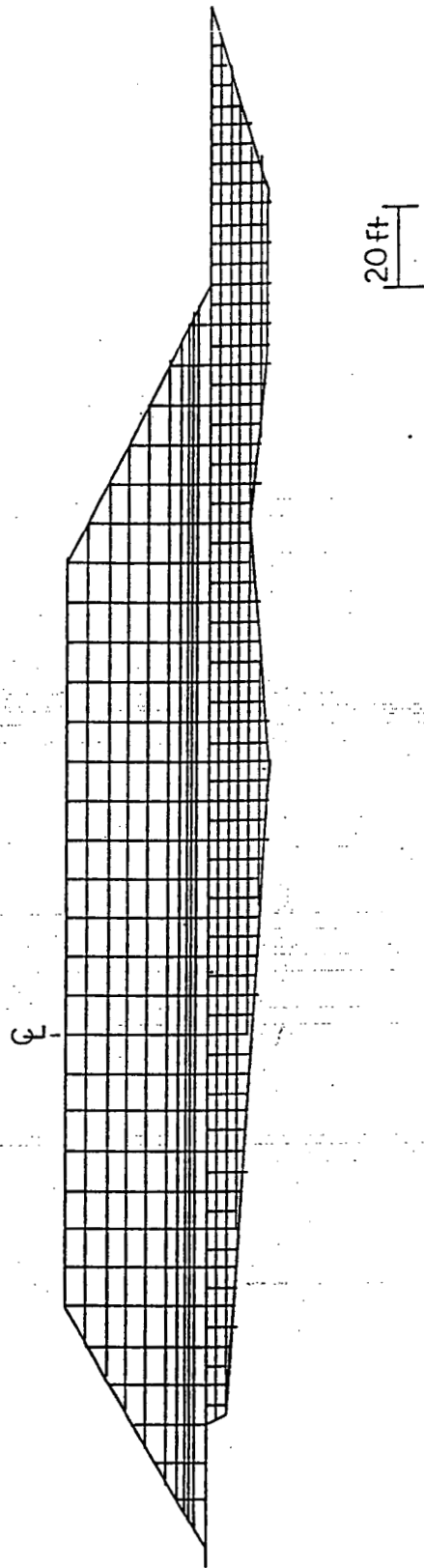


Fig. 4.1a. FEM Mesh, Sta. 397

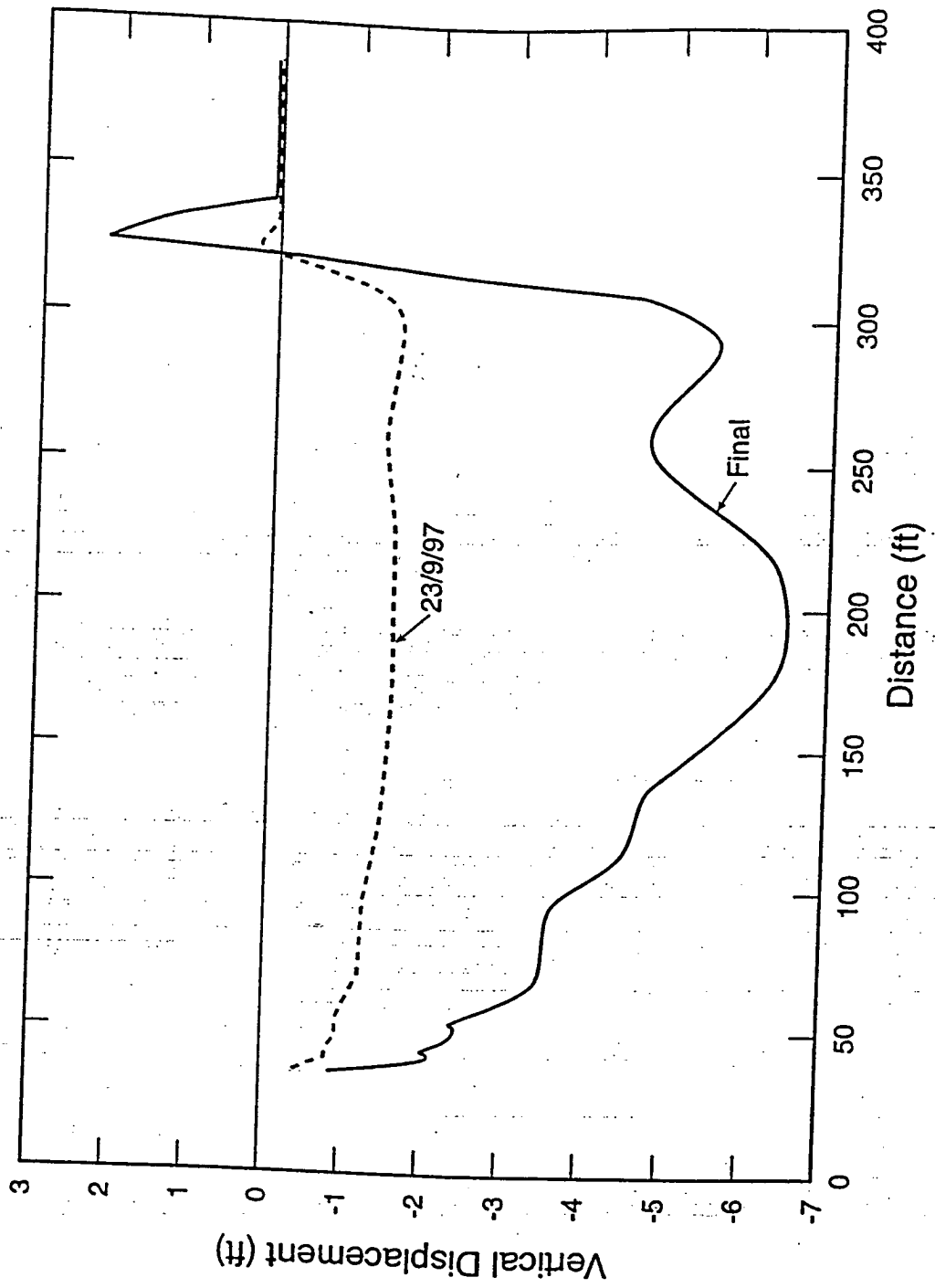


Fig. 4.1b. Vertical Displacements Computed by FEM, Sta. 397. Negative displacement indicates downward movement or settlement. Centerline is at distance 160 ft.

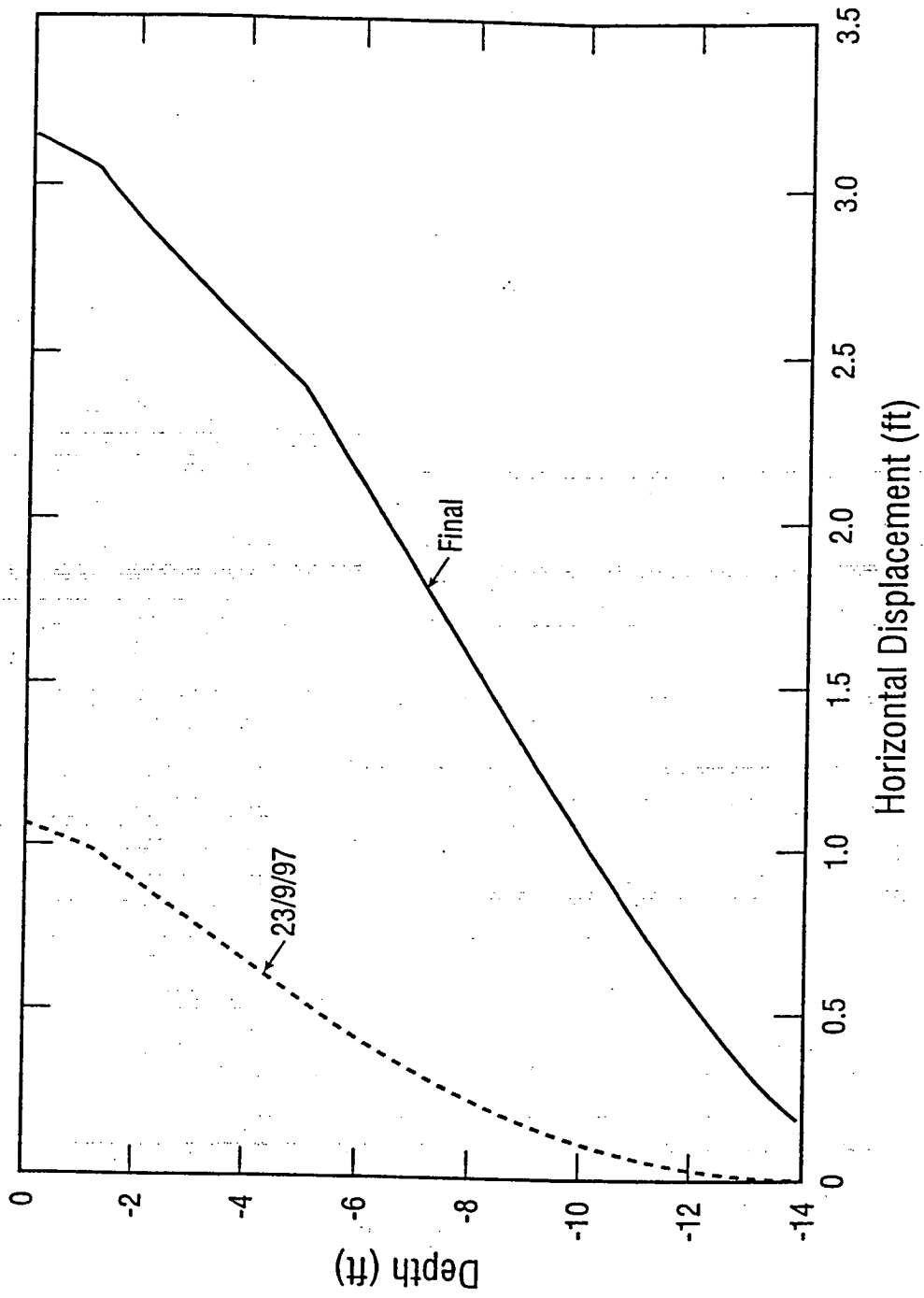


Fig. 4.1c. Horizontal Displacements Computed by FEM, Sta. 397

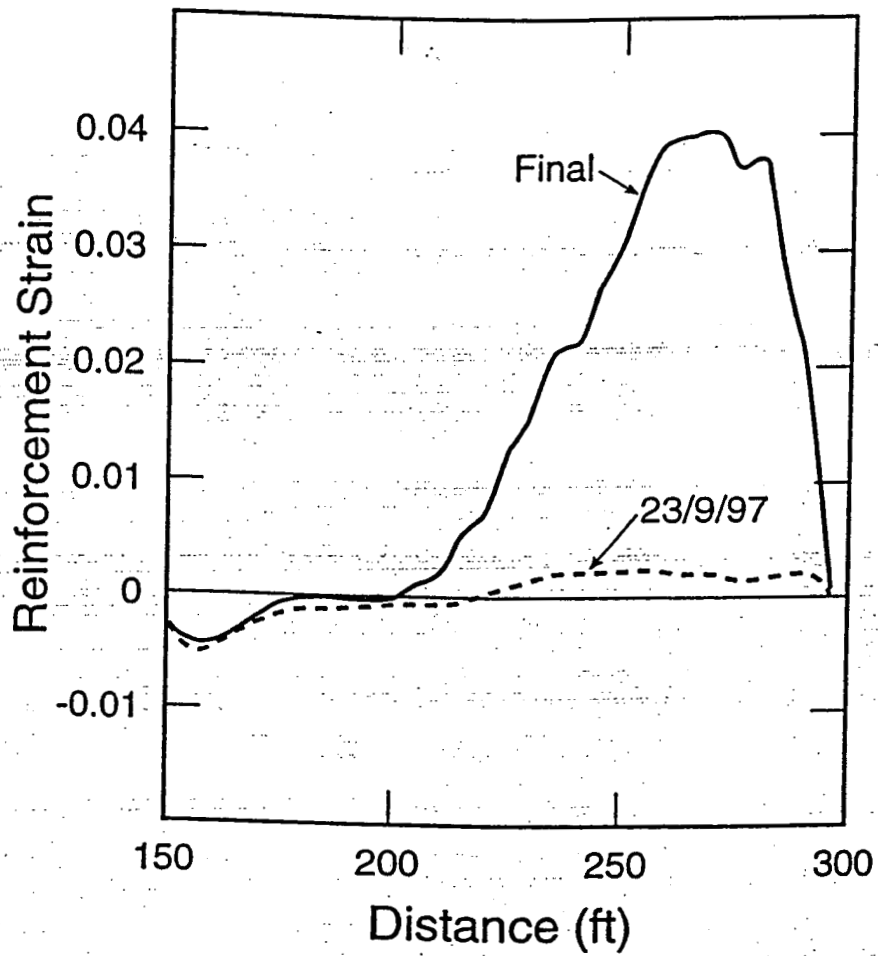


Fig. 4.1d. Reinforcement Strain Computed by FEM, Sta. 397. Centerline is at distance 160 ft.

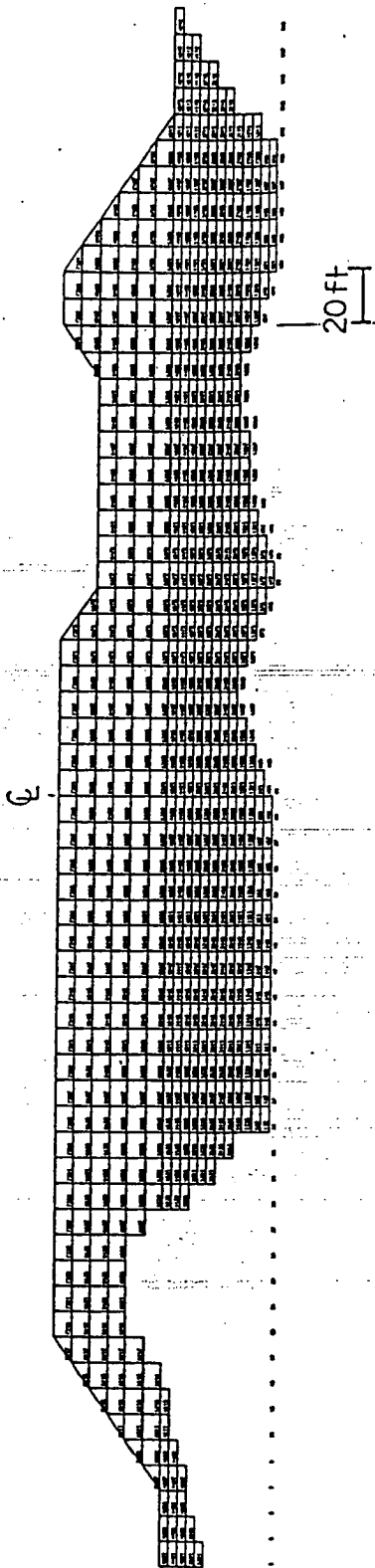


Fig. 4.2a FEM Mesh, Sta. 395

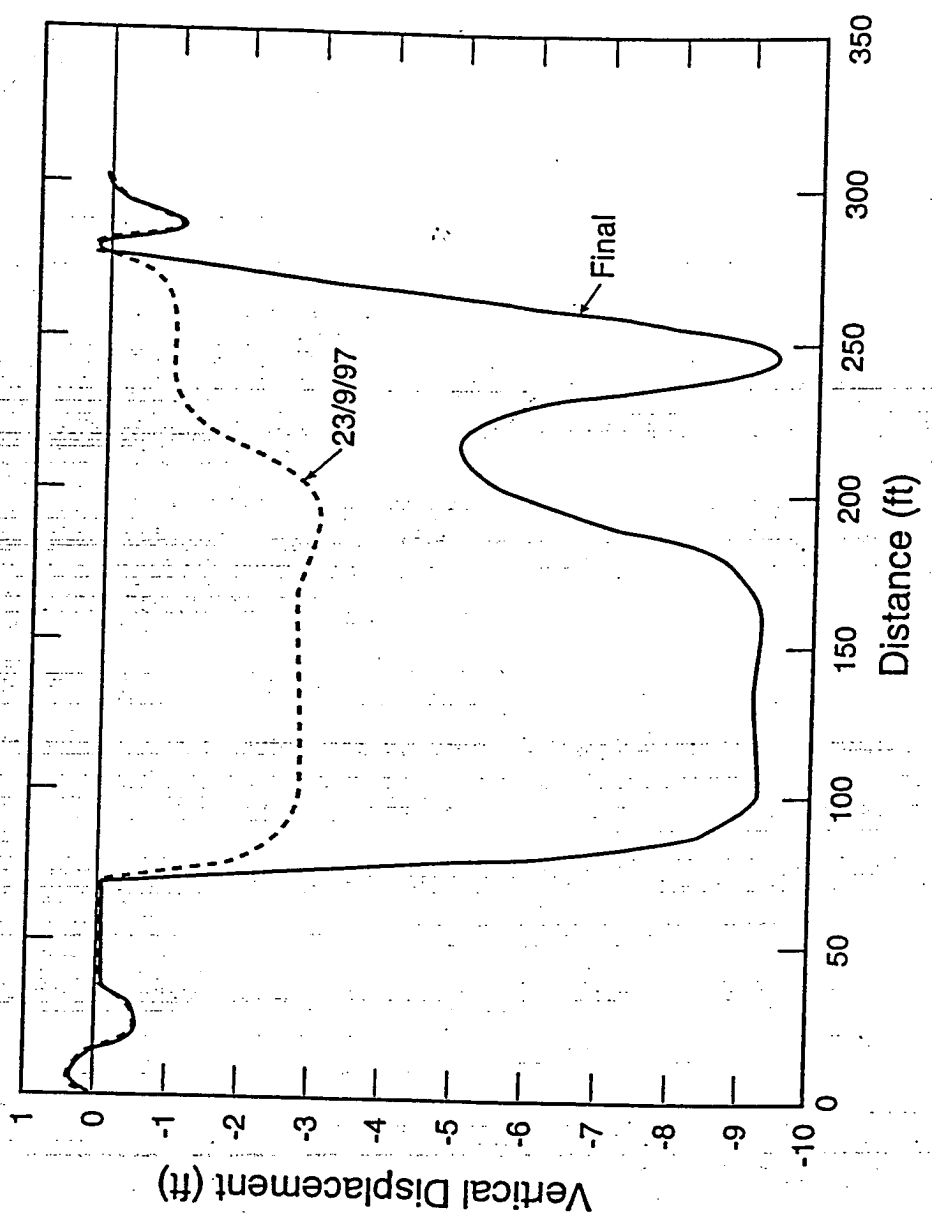


Fig. 4.2b. Vertical Displacements Computed by FEM, Sta. 395. Negative displacement indicates downward movement or settlement. Centerline is at distance 315 ft.

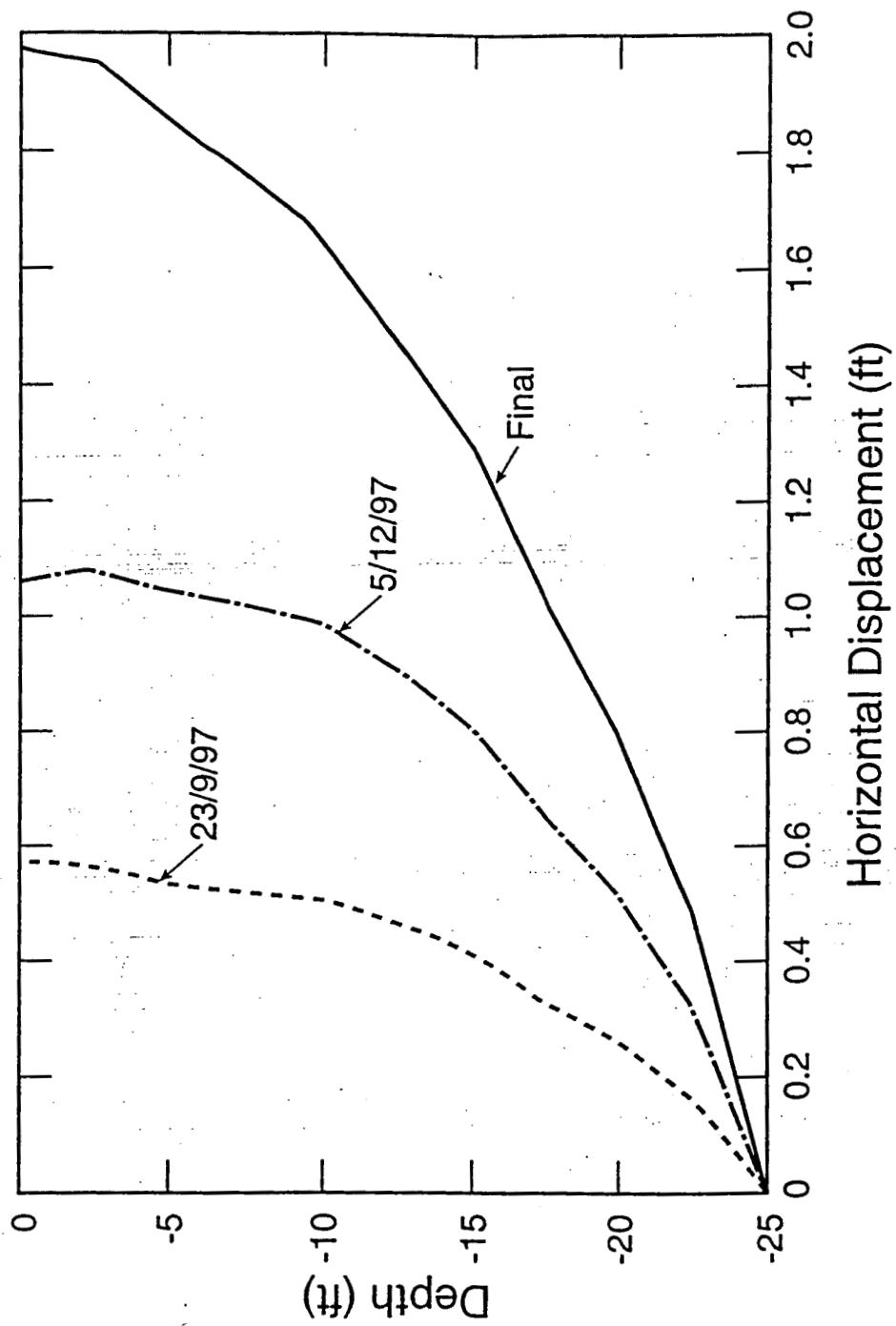


Fig. 4.2c. Horizontal Displacements Computed by FEM, Sta. 395

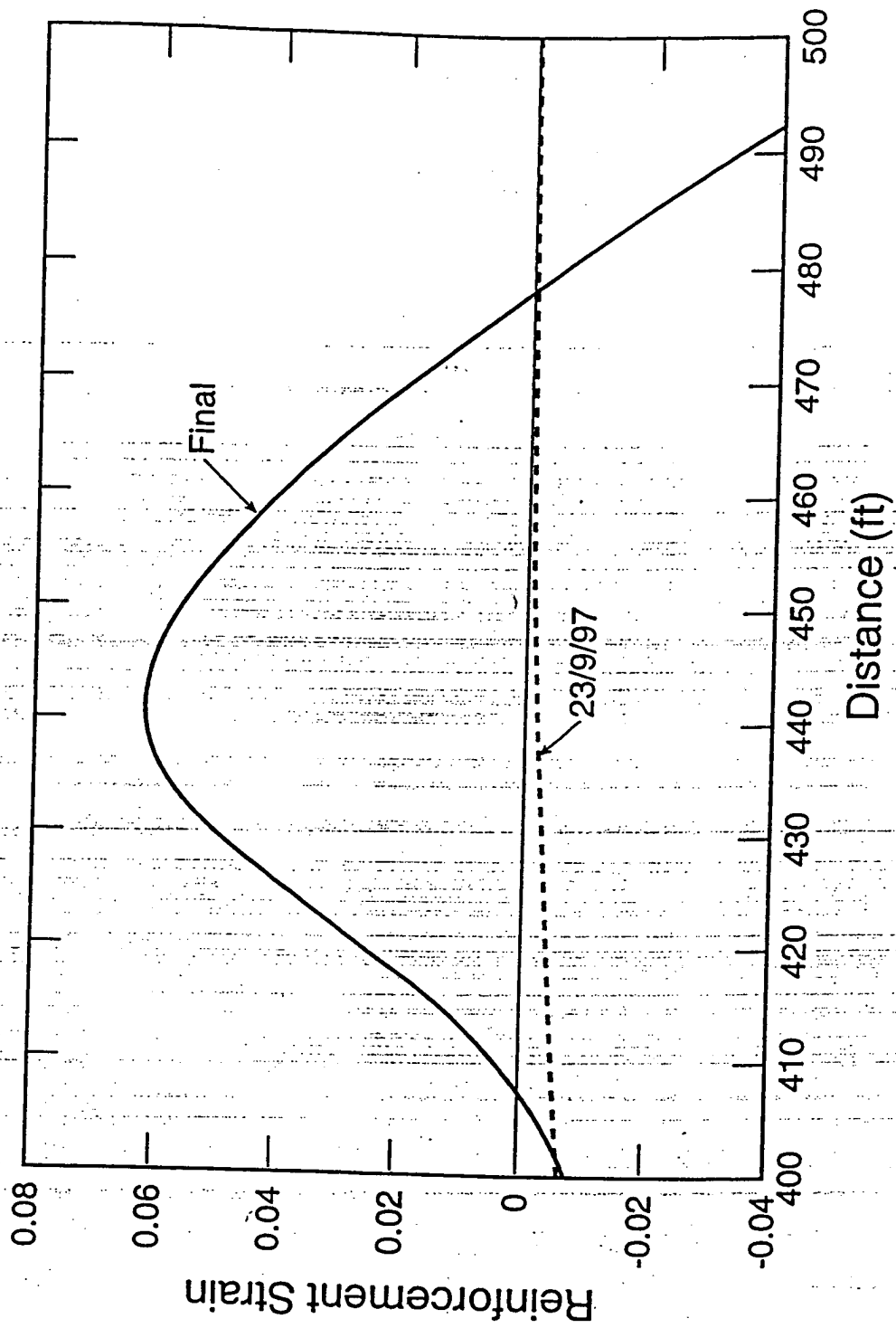


Fig. 4.2d. Reinforcement Strain Computed by FEM, Sta. 395. Centerline is at distance 315 ft.

Table 4.5. Calculated and Measured Vertical Settlements

Station	Location	Embankment height ¹ (ft)	Sludge thickness (ft)	Calc. Settl. (ft)	Meas. Settl. (ft)	Ratio Calc./Meas.
395	ct	30	26	² 6.0	4.13	0.68
395	20 rt (SA)	32	25	² 7.0	8.16	1.16
397	20 (10)rt (SA)	32	15	² 3.0	3.48	1.16
400	ct.	32	27	9.29	8.40	1.10
401	cl	30	18	1.60	2.43	0.65
402	cl	28	22	7.32	7.78	0.94
403	cl	27	26	8.17	7.76	1.05
404	cl	22	12	4.00	2.16	1.85
405	cl,	23	7	2.88	2.32	1.24
407	cl,	25	18	5.90	4.85	1.22
408	cl,	24	24	7.75	7.00	1.10
409	cl	26	22	7.20	6.54	1.10

¹ This is the distance between ground surface and top of embankment. The load used to calculate settlement includes the fill added to compensate for the settlement. ² Calculated by FEM.

4.4. Horizontal Displacement

The horizontal displacements calculated by FEM are shown in Fig.4.1c and 4.2c. The calculated displacement has the maximum at the ground surface and these values are given in Table 4.6. The measured displacements at Sta. 392, 395, and 406, as shown by the plots in Appendix A, show a maximum at some depth below the ground surface. These maximum displacements are also given in Table 4.6. We note that measurement of the horizontal displacement did not start until 17, Dec. 97. For comparison, the difference between the displacements calculated for 5, Dec., 97 and the final state should be used. We see that the calculated displacement at the ground surface of Sta. 395, which is 0.9 ft (= 1.96-1.06), is much

larger than the measured displacement of 0.3 ft but is close to the maximum measured displacement of 0.9 ft.

Sta. 395 is the only location where both calculated and measured displacements are available. However, for a general comparison, we can compare the calculated displacement at Sta. 395 and 397 with the measured displacements at Sta. 392, 395 and 406. The general conclusion is that the calculated displacements are too large. The measured displacement at Sta. 409 is considerably smaller than those at the other stations. We attribute this to the higher strength of the sludge as shown in Sec. 4.6.

Table 4. 6 Calculated and Measured Horizontal Displacements

Station s	Location	Date (day,mo,yr)	Calculated Displace- ments (ft)	Measured Displacements(ft)	
				Gr. surf.	Max.
392	50 rt	10,2,99		0.75	1.0
395	65 rt	5,12,97	1.06	0	0
395	65 rt	22,7,98	1.97	0.30	0.92
397	200 rt	23,9,97	1.0	Not measured	
397	200 rt	Final	3.2	Not measured	
406	125 rt	25,11,99		0.3	0.70
409	115 lt.	10,2,99		0.25	

4.4. Reinforcement Strain

The strains in the reinforcement as calculated by FEM are shown in Fig.4.1d and 4.2d. Note that the strain varies over a large range with distance. The maximum calculated strain for Sta. 397 is located approximately below the top of the slope. This agrees with many earlier studies (Wu, 1996). However, the maximum calculated strain for Sta. 395 is located well to the left of the top of the slope. This may be due to the irregular bottom of the sludge deposit because the calculated strain is sensitive to the profile of the sludge bottom.

Table 4.7 gives the measured strains between pairs of wire extensometers, with their locations given as distances (ft) from the toe of the embankment slope. For each station, the average of the measured strains for all extensometer pairs on all three reinforcement layers are given as the average for the distance covered by all the extensometer pairs. This serves as a general measure of reinforcement strain because the measured strains show considerable scatter

and there do not appear to be any consistent difference between the strains in the three reinforcement layers. For Sta. 395, the measured strains for different extensometer pairs are listed separately. These are compared with the calculated strains for the same locations. The calculated strains are larger than the measured strains but show the same pattern. The strain is large between 17 and 87 ft from the toe but much smaller at greater distances. The calculated strain for Sta. 397 is also shown for comparison. The strains show the same pattern as those for Sta. 395 but are smaller because of the smaller sludge thickness. The measured strains at the other stations are considerably smaller. The reasons for the smaller strains could be smaller embankment height or smaller sludge thickness. The limited scope of the project did not permit investigation of this issue.

Table 4.7 Calculated and Measured Reinforcement Strains

Station	Location (ft)	Calculated strain	Measured strain
394 + 80, rt	17-130		ave. = 0.008-0.011
	17-52	0.020	0-0.009
	52-87	0.040	0.016-0.020
	30-80	0.040	0.017
	80-130	0	0.001
397	17-52	0.030	not measured
	52-87	0.015	not measured
	30-80	0.030	not measured
	80-130	0.002	not measured
400 + 15, lt	30-130	not computed	ave. = 0.0025-0.0045
403 + 85, rt	30-130	not computed	ave. = 0.0045-0.0065
409+15, lt	30-130	not computed	ave. = 0.0065-0.0070

4.5. One-dimensional Compression

The vertical displacement, or settlement, can also be estimated using the assumption of one-dimensional compression (Terzaghi, 1943). The compression for a layer i is

$$v_i = \frac{C_r}{1 + e_0} \{ \log \sigma'_p - \log (\sigma'_0 + 3\gamma) \} h_i + \frac{C_c}{1 + e_0} \{ \log \sigma'_1 - \log \sigma'_p \} h_i \quad [4.4a]$$

when $(\sigma'_0 + 3\gamma) < \sigma'_p$ or

$$v_i = \frac{C_c}{1 + e_0} \{ \log \sigma'_1 - \log (\sigma'_0 + 3\gamma) \} h_i \quad [4.4b]$$

when $(\sigma'_0 + 3\gamma) > \sigma'_p$ and the settlement at the ground surface is

$$v_0 = \sum v_i \quad [4.4c]$$

where C_r , C_c = recompression and compression indices, e_0 = initial void ratio, h_i = thickness of layer i

The quantity $(\sigma'_0 + 3\gamma)$ was used as the initial condition because all settlement measurements were started after the working platform was finished. The exception is Sta. 405 where the surface was near el. 716 at the initiation of settlement measurements. At this station, the initial condition $(\sigma'_0 + 6\gamma)$ was used. The settlement was calculated with the updated preconsolidation pressures σ'_p given in Table 4.4, with the exception of Sta. 401. This is the location of the test embankment and the sludge has been consolidated under the weight of the test embankment. The vertical stress due to the weight of the test embankment is between 2500 psf (120 kPa) at the top of the sludge and 1500 psf (72 kPa) at the bottom of the sludge. This was added to $(\sigma'_0 + 3\gamma)$ to give the preconsolidation pressure for Sta. 401.

Because of the high compressibility (C_c), the assumption of small strain used in Eq. [4.4] does not apply. Large strain analysis has been described by Argyris (1965) and Carter et al (1977), among others. A simplified version was used here. The compression v_i is calculated for increments of pressure. The compression due to each pressure increment is subtracted from the layer thickness to obtain the reduced thickness. The reduced thickness is then used as h_i in the calculation for the next pressure increment. Similar correction was used to obtain e_0 . The calculated settlements are given in Table 4.5.

Only settlements at the centerline were computed, because at points on the shoulder or the slope the loading is not uniformly distributed and the condition of one-dimensional compression is not satisfied. In addition, settlements at Sta. 395, 397, 398 and 406 were not computed because of large irregularities on the bottom of the sludge. This may be seen in Fig. 3.2 for Sta. 395, Fig. 3.3 for Sta. 397, and Fig. 3.4 for Sta. 406. The large irregularities also violate the condition of one-dimensional compression.

The ratios of calculated to measured settlements are shown in Table 4.5. With the exception of Sta. 404, the ratio falls within the range of 0.65-1.25. This means that the one-dimensional method has an accuracy of $\pm 35\%$. The condition at Sta. 404 is unusual in that very small porepressures were measured in both piezometers and the porepressure response to loading was erratic. While this could mean that the piezometers were not functioning properly, it could also mean that the sludge had a higher preconsolidation pressure. This could lead to a smaller settlement. This question cannot be resolved with the available data and Sta. 404 is considered to be an exception.

4.5. Undrained Shear Strength

One of the issues during design is the gain in the strength of the sludge following consolidation. Eq.[3.1] gives an approximate estimate of the undrained shear strength. During construction, vane shear tests were performed to measure the undrained shear strength at different times. To verify the design procedure, we attempt to predict the vane shear strength using the results of triaxial tests performed prior to design and construction. The strength measured in vane shear tests can be estimated as follows.

The first procedure uses the total stress and is similar to Eq.[3.1]. It ignores the effect of stress state on the undrained shear strength, defined as

$$s_u = (\sigma_1 - \sigma_3) / 2 \quad [4.5]$$

where σ_1, σ_3 = major and minor principal stresses, respectively. Then s_u measured in the vane shear test is the same as s_u measured in the triaxial test. It follows that

$$s_u = \sigma_{3,c} \sin \phi / (1 - \sin \phi) \quad [4.6]$$

where $\sigma_{3,c}$ = consolidation pressure, ϕ = angle of internal friction in total stress, in the consolidated-undrained triaxial test.

The alternative is to use the effective stress analysis which allows consideration of the difference in stress states between the triaxial test and the vane shear test. The stresses on the failure surface in the vane shear test are shown in Fig. 4.3a, where $\sigma_z, \sigma_r,$ and σ_θ = vertical, radial, and tangential stresses, respectively. The undrained shear strength is

$$s_{u,v} = (\sigma_{r,c}' - \alpha \Delta \tau_o) \tan \phi' \quad [4.7]$$

where $\sigma_{r,c}'$ = effective in-situ radial stress after consolidation, α = porepressure parameter, τ_o = octahedral shear stress and Δ denotes change during the vane shear test, ϕ' = angle of internal friction in effective stress. In the vane shear test,

$$\Delta \tau_o = \frac{1}{3} [(\Delta \sigma_1 - \Delta \sigma_2)^2 + (\Delta \sigma_2 - \Delta \sigma_3)^2 + (\Delta \sigma_3 - \Delta \sigma_1)^2]^{1/2} \quad [4.8]$$

where σ_2 = intermediate principal stress. If we ignore the curvature of the failure surface, the stress changes during the vane shear test can be shown on the Mohr's circle in Fig. 4.3b. From this, we get

$$\Delta\sigma_1 = -\Delta\sigma_3 = s_{u,v} - \frac{1}{2}(\sigma_{\theta,c}' - \sigma_{r,c}') \quad [4.9]$$

where $\sigma_{\theta,c}'$ = effective in-situ tangential stress after consolidation. For $\sigma_{r,c}' = \sigma_{\theta,c}'$, we obtain

$$s_{u,v} = \frac{\sigma_{rc}' \tan \phi'}{1 + 0.8\alpha \tan \phi'} = \frac{\tan \phi'}{1 + 0.8\alpha \tan \phi'} K_0 \sigma_z' \quad [4.10]$$

where σ_z' = vertical effective stress after consolidation, K_0 = coefficient of earth pressure at rest.

The undrained shear strength of the sludge after consolidation was estimated from the strength properties using both total stress and effective stress methods, using Eq. [4.6] and [4.10], respectively. The total stress prediction was made using 0.53 for $\sin \phi / (1 - \sin \phi)$. This is the average from 11 triaxial tests performed for the preceding project. The value of $\sigma_{3,c}'$ was taken to be the embankment weight plus the overburden pressure at the middle of the sludge layer. For the effective stress method,

$$K_0 = 1 - \sin \phi' \quad [4.11]$$

and $\phi' = 45^\circ$, $\alpha = 0.7$ were used in Eq. [4.10]. These are also the average of the 13 triaxial tests. The computed undrained shear strengths are given in Table 4.8.

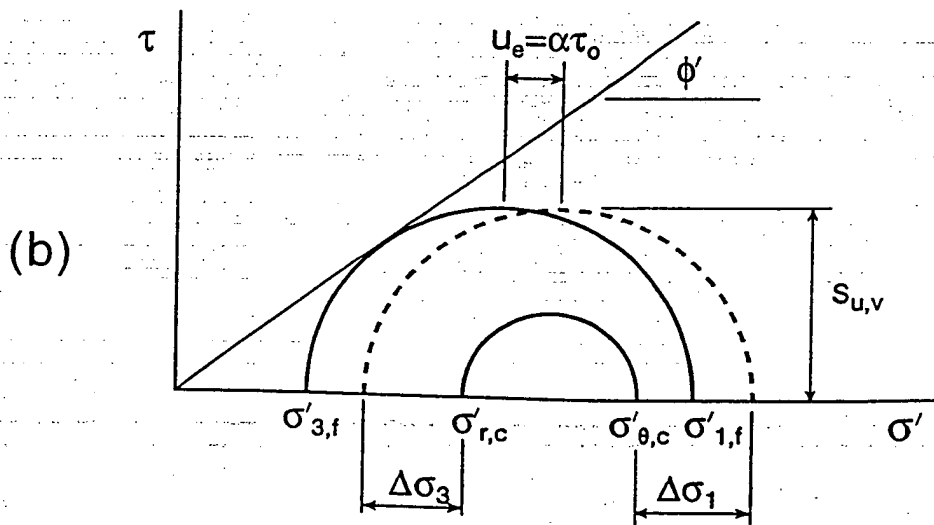
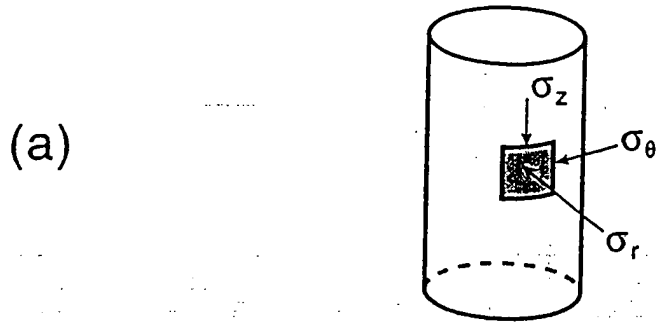


Fig. 4.3a. Mohr's Circle of Stress for Vane Shear
 Fig. 4.3b. Measured Vane Shear Strengths

Table 4.8. Calculated and Measured Shear Strengths

Method	Condition	Calculated s_u		Measured s_u	
		(psf)	(kPa)	(psf)	(kPa)
Total stress	Initial state	450	21.6	150	7.2
	Final state	1910	91.7	1150-1300	55-62
Effective stress	Initial state	172	8.3	150	7.2
	Final state	896	43.0	1150-1300	55-62

The measured vane shear strengths at various times during construction are plotted in Fig. 4.4. Also shown are the ranges in the vane shear strength measured before construction. The measured strengths at Sta.395 on 7, Oct., 97 are very close to the strength measured before construction, indicating no gain in strength from the 3 ft.(0.9m) of fill that constitutes the working platform. The strength measured on 27, Oct, 97, showed a slight increase, as embankment construction had reached elevation 717. The strengths measured on 13, Oct,98 at Sta. 395 and 402 represent the strength after consolidation under the full load. The values at the middle of the sludge deposit are given in Table 4.8. The value for the initial state represent the the strength at Sta. 395-402. This is because the sludge properties used for prediction were derived from laboratory tests performed on samples from this section. The initial strength shown for Sta. 410-412 indicate a higher strength for this section.

We see that the total stress method overestimates the initial and final strengths while the effective stress method makes a reasonably good estimate of the initial and final strengths. The measured initial and final strengths are 0.30 and 0.64 of the strengths predicted by the total stress method, and 1.0 and 1.4 the strengths predicted by the effective stress method. We should note the large scatter in the measured final strength and also the small number of vane shear tests performed. Hence, the comparison is not entirely conclusive. In our opinion, the results show that the methods can be used to estimate the order of magnitude of the final strength.

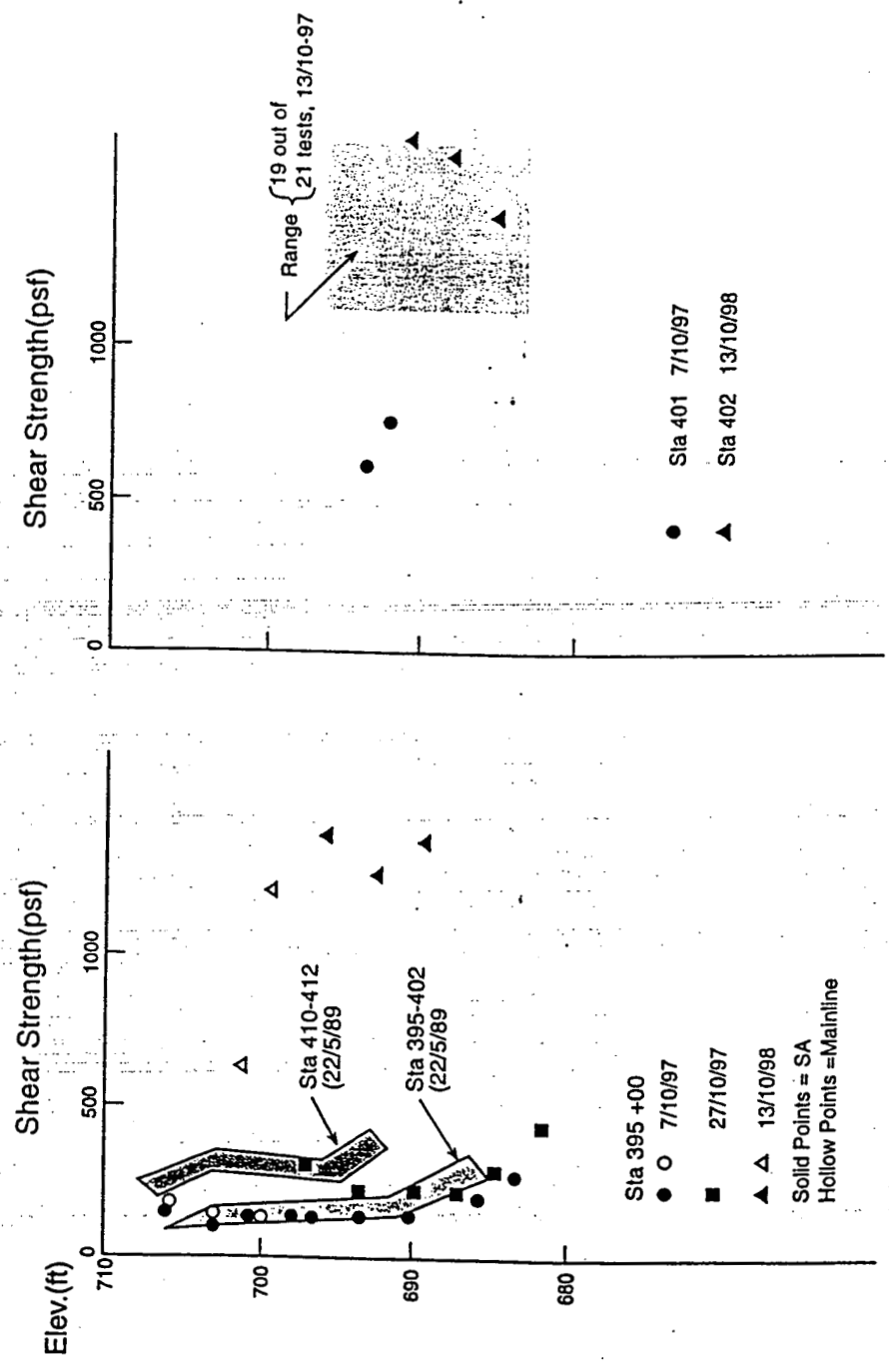


Fig. 4.4. Measured Vane Shear Strengths

5. CONCLUSIONS AND RECOMMENDATIONS

The general conclusion is that the performance of the full-scale embankment is close to what was expected at the design stage. Therefore, we consider the method used in the design of the embankment are sound and the results obtained from the test embankment can be used to obtain a satisfactory prediction of the performance of the full-scale embankment. Specifically, we find the following:

1. The rate of consolidation as reflected by the measured porepressures is of the same order of magnitude as that estimated by the radial consolidation theory, using the coefficient of consolidation measured in laboratory consolidation tests. Thus, the laboratory results and consolidation theory can provide a reliable estimate of the rate of consolidation in the sludge. This can also be interpreted to mean that the wick drains performed effectively in the sludge.
2. The finite element method (FEM) gives a good estimate of the vertical displacement. It overestimates the horizontal displacement by about 50%. The FEM also overestimates the reinforcement strains by about 50% at Sta. 395. This difference in calculated and measured reinforcement strain need to be viewed in the context of the overall small magnitude of both calculated and measured strains, relative to the design strain. Both calculated and measured strains are below 0.04, while the design strain is 0.10.
3. The one-dimensional compression method gives a good prediction of the vertical displacement near the center of the embankment.
4. The effective stress method gives a good prediction of the initial strength of the sludge and the strength after consolidation. The total stress method overestimates both the initial strength and the strength after consolidation. The two methods, when used together, can provide an order-of magnitude estimate of the strength after consolidation.
5. Overall, the prediction methods used here can estimate the right order of magnitude of consolidation rate, displacement, strain, and strength to an accuracy of 50 % or better.

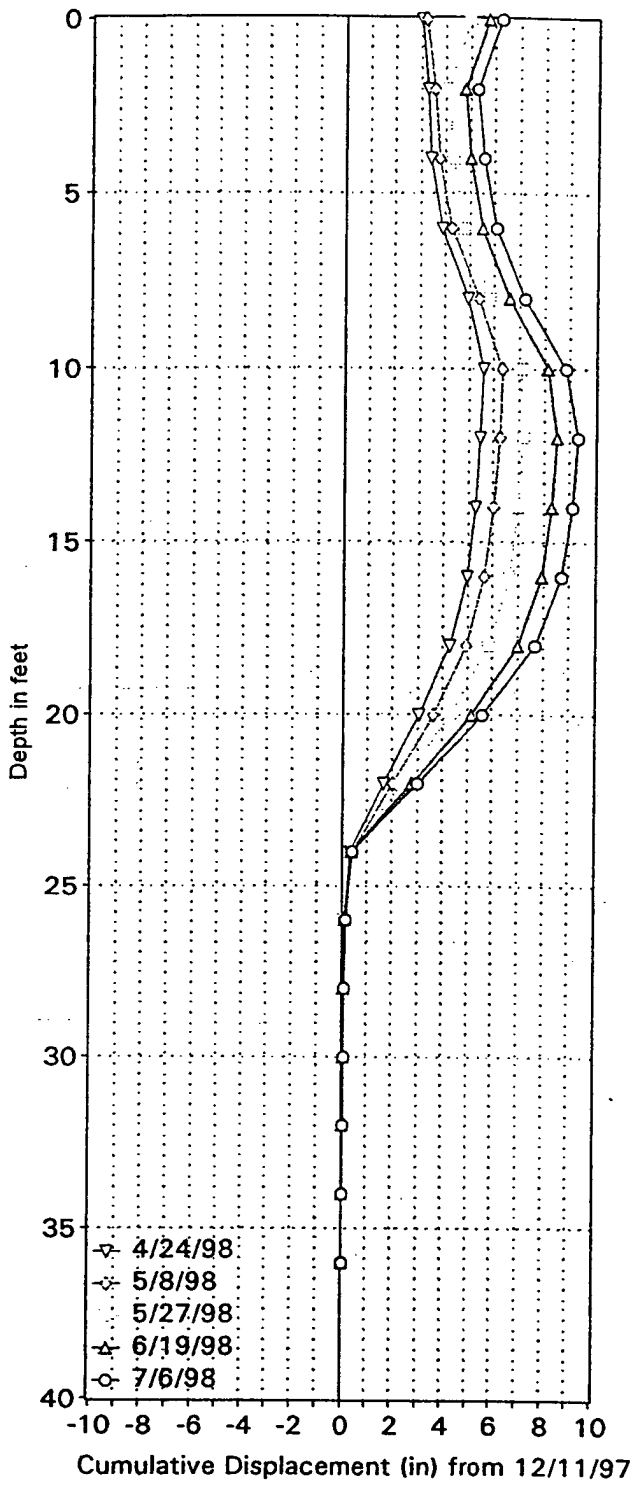
Our recommendation is that the procedures used in the measurement of material properties, the design of the embankment, the prediction of embankment performance and the use measurements during construction for construction control provide an effective methodology that can be applied to the design and construction of other reinforced-soil embankments over soft ground.

6. IMPLEMENTATION

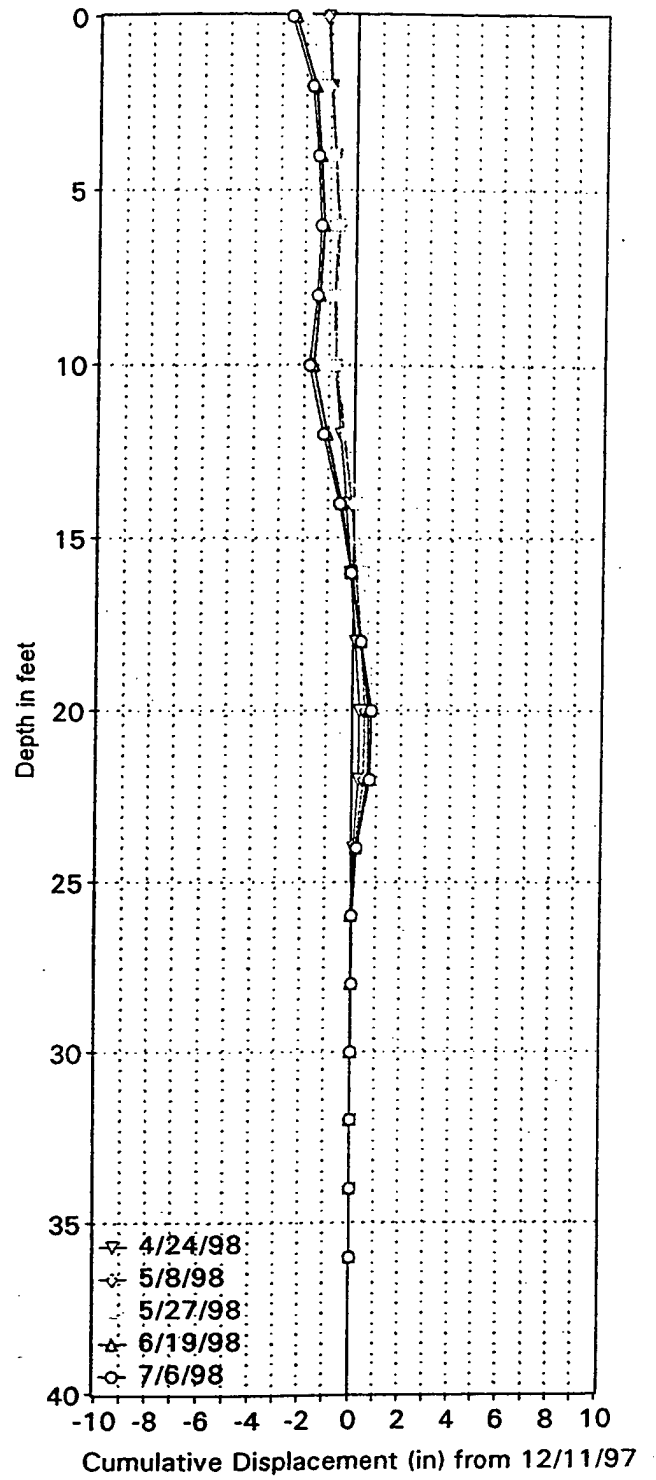
The results of this project can be implemented through the use of the procedures developed here for the design and construction of future projects. The general approach of using a test embankment to verify critical design assumptions and careful monitoring of performance during construction as a part of construction control has proven to be successful. More specifically, the laboratory tests, the methods for estimating rate of consolidation, strength after consolidation, and stability, and the program for monitoring embankment performance for construction control can be implemented in future projects involving embankments on soft ground. This report and the related reports (Wu, 1996; Gale, 1998, 1999) can serve as reference material for future projects.

APPENDIX A. MEASURED SETTLEMENT, POREPRESSURE, HORIZONTAL DISPLACEMENT
AND REINFORCEMENT STRAIN

06083 2, A-Axis



06083 2, B-Axis

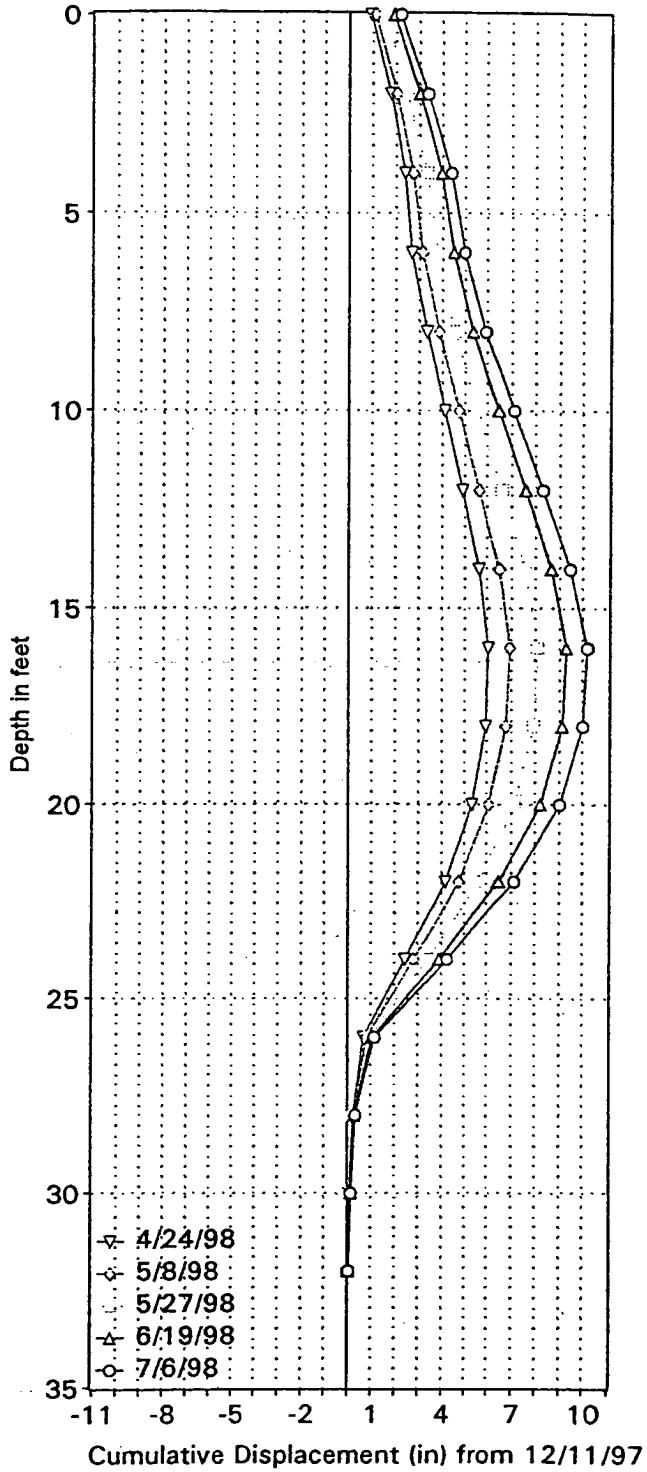


FRA-670-1.14

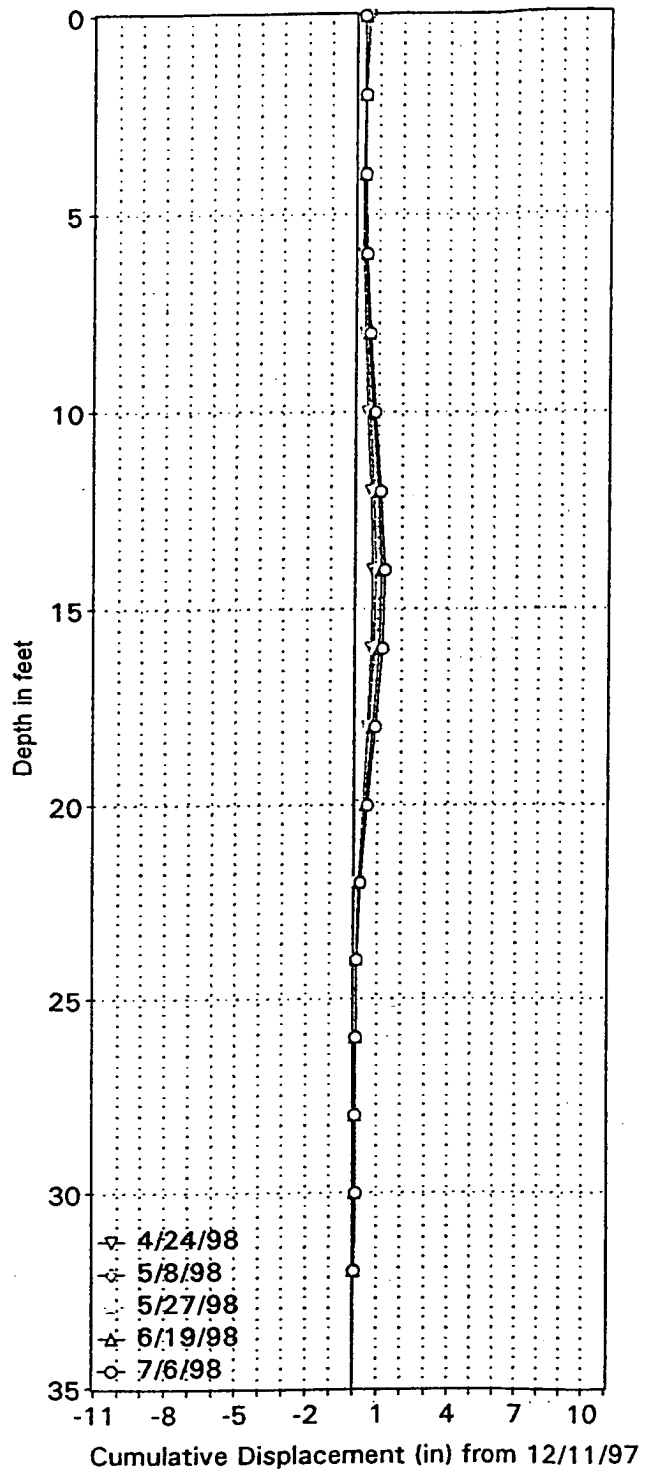
Installation #2

Sta. 392+00, 50' Rt.

06083 3, A-Axis



06083 3, B-Axis

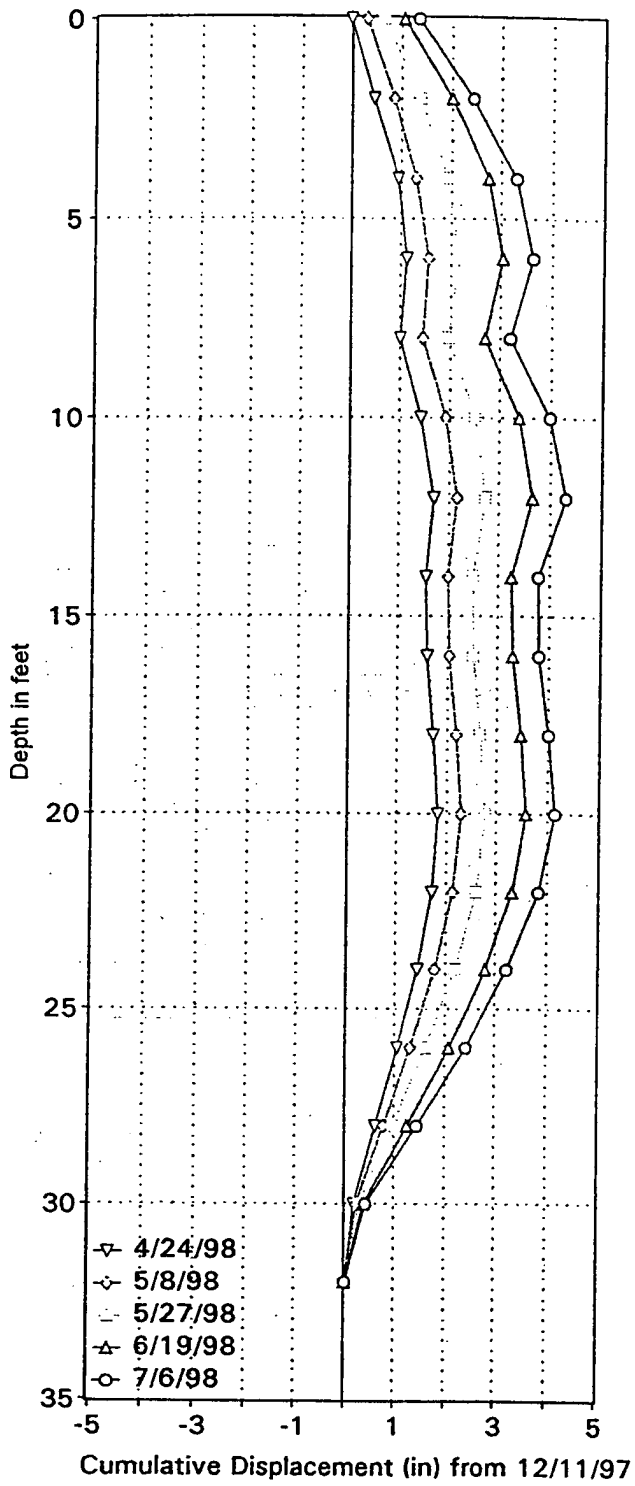


FRA-670-1.14

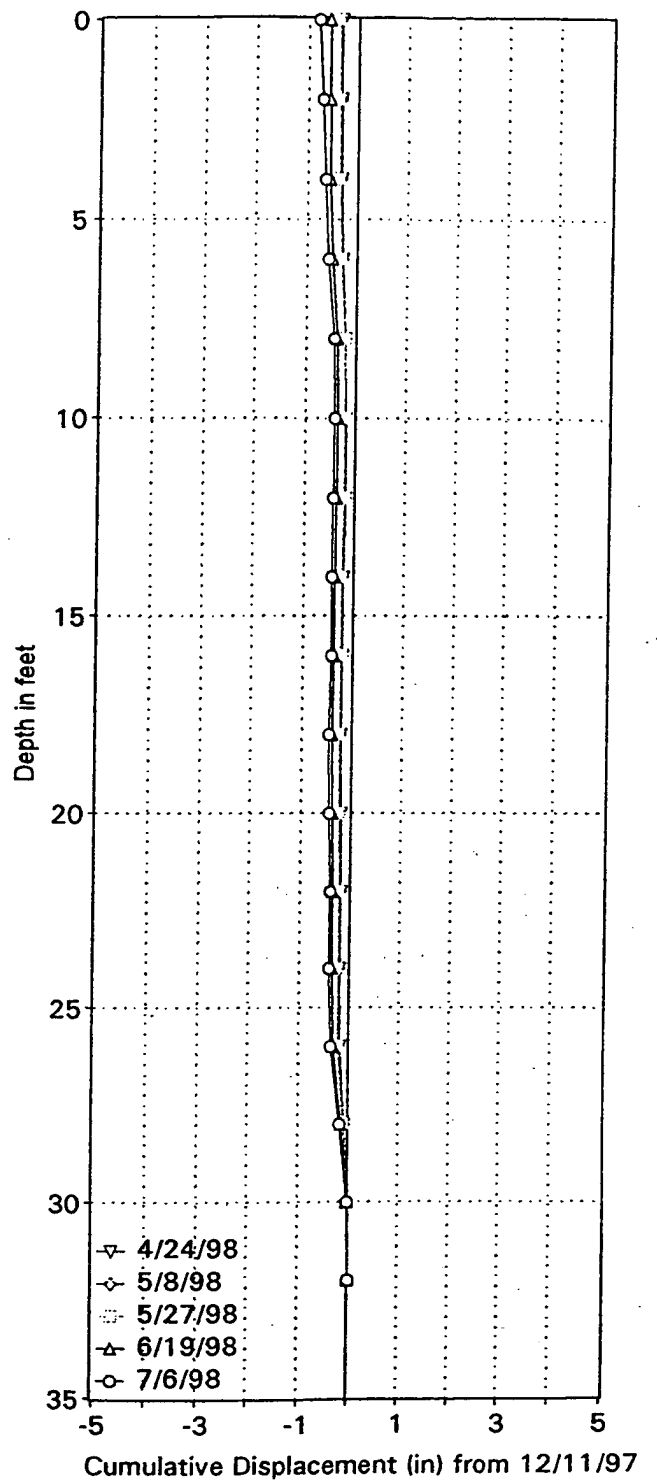
Installation #3

Sta. 395+00, 65' Rt.

06083 4, A-Axis



06083 4, B-Axis

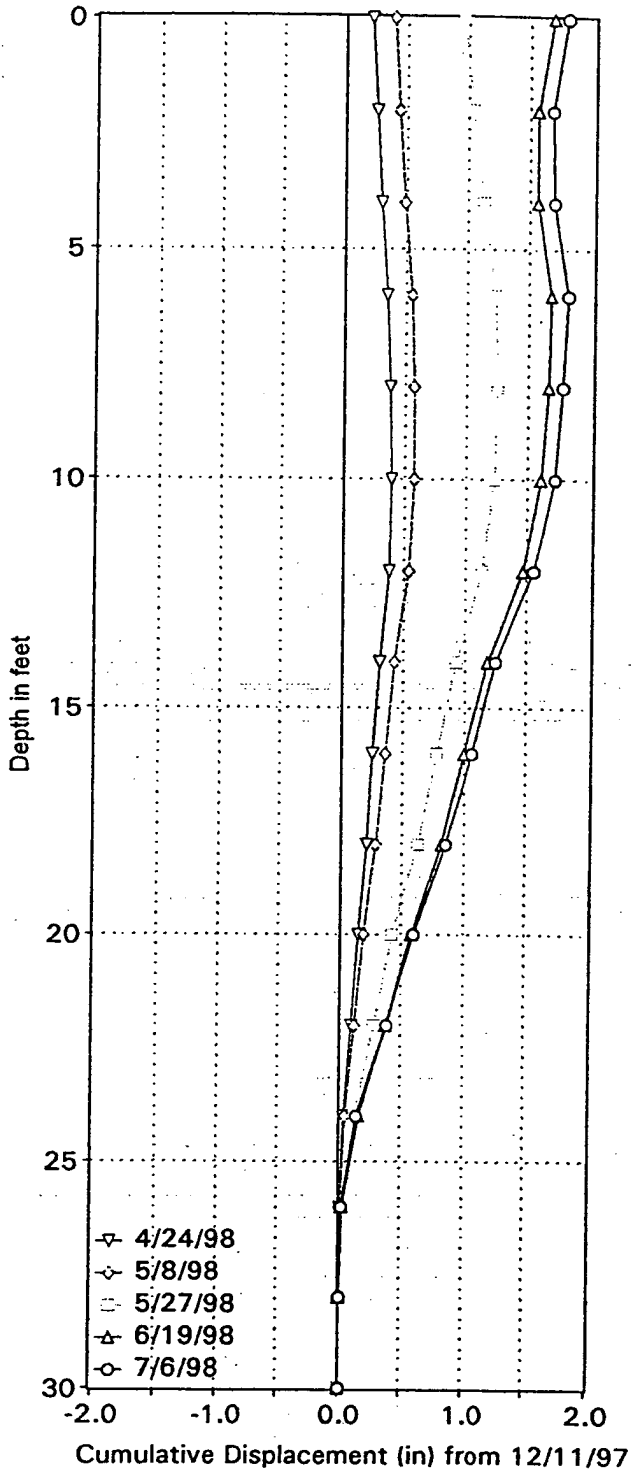


FRA-670-1.14

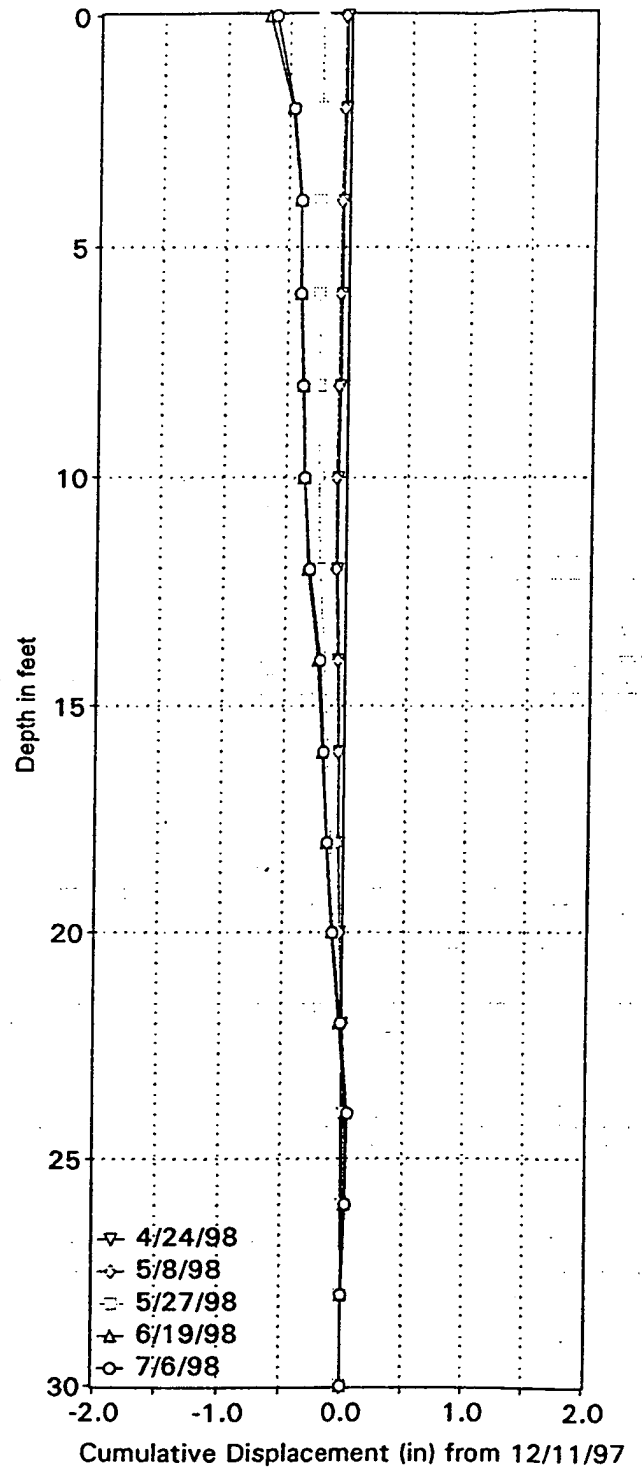
Installation #4

Sta. 406+00, 125 Rt.

06083 5, A-Axis



06083 5, B-Axis



FRA-670-1.14

Installation #5

Sta. 409 +00, 115 Lt.

APPENDIX B. SOLUTION FOR TIME-DEPENDENT LOADING

Schiffman's (1958) solution for radial drainage under time-dependent loading is shown here as Fig. B.1.

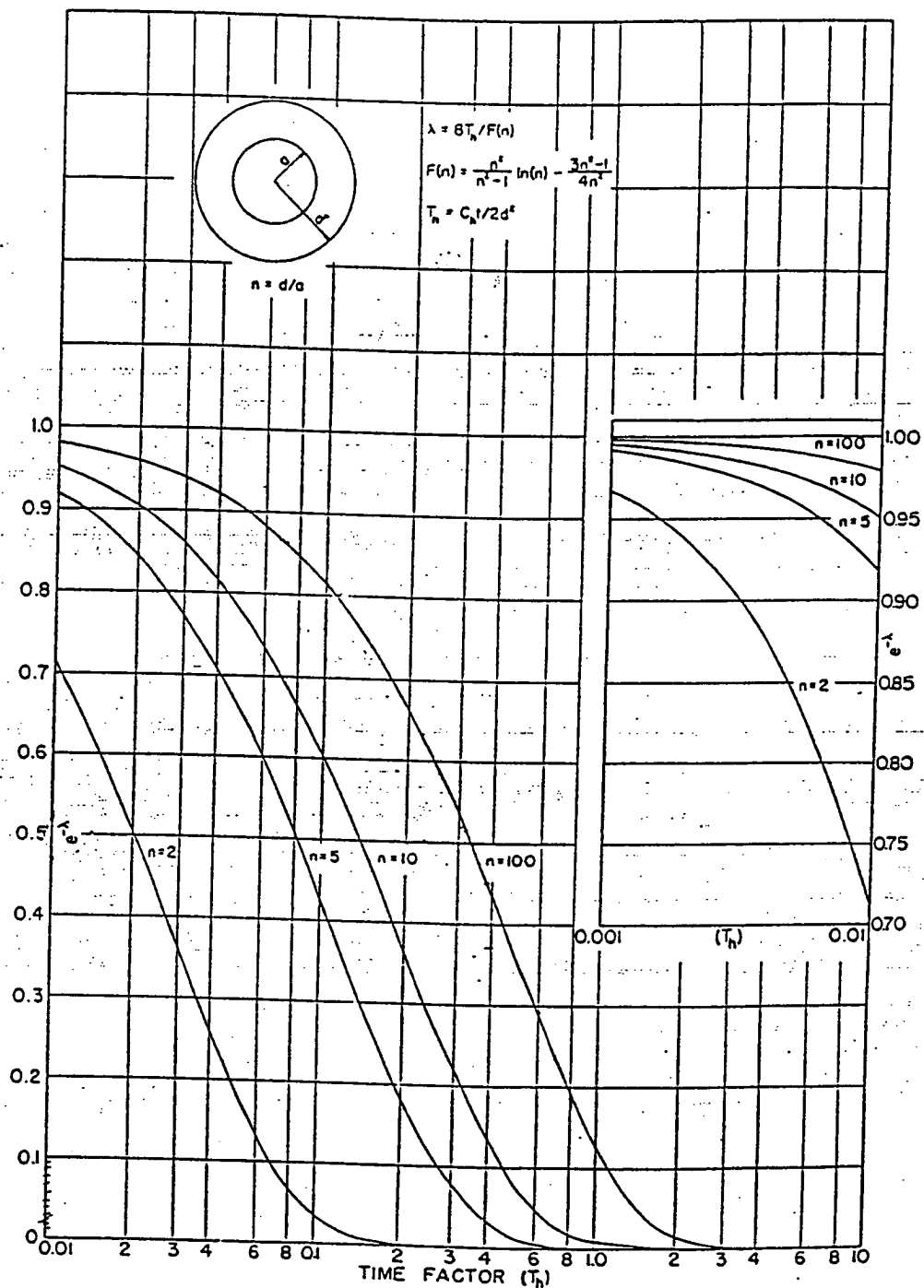


Figure 21. Exponents for equal-strain sand-drain problems, no smear, radial flow.

Fig. B.1 Solution for Radial Drainage with Time-Dependent Loading (Schiffman, 1958).

APPENDIX C. UPDATING WITH OBSERVED PERFORMANCE

The observed performance of the test-embankment was evaluated with methods of system-identification (Schweppe, 1973) which provides a systematic means for comparison of observed performance with predicted performance and can account for uncertainties in input, output, and observation. In system identification, the performance (s) is expressed as a function (H) of the input parameters (x) and an error v ,

$$s = H(x) + v \quad [C.1]$$

H is the prediction model and represents the finite element method (FEM) in this case history. The observed performance (z) is

$$z = s + w \quad [C.2]$$

where w is the observational error. System identification method provides a means to get the best estimates of s ($=s''$) and x ($=x''$) from the observed performance z and the estimated errors or uncertainties in x and z and the uncertain errors v and w .

The solution is expressed as

$$x'' = G(z, v, w, H') \quad [C.3]$$

where G is the inverse solution, and H' is the sensitivity of the performance (s) to the input parameters (x). Eq. [C.3] gives the best estimate of x ($=x''$) from the observed results and x'' is called the updated value of x .

This solution scheme includes all the key elements of geotechnical design. For example, the elements of s ($=s_j$) may be vertical displacement or geotextile strain, and the elements of x ($=x_j$) may be compressibility or preconsolidation pressure. The procedure for updating and computing sensitivity has been developed by Zhou (1995). In addition, Zhou (1995) gives a procedure for back-calculation of x from z , which is the solution of Eq. [C.3], and the updated parameters for the test embankment.

APPENDIX D. REFERENCES

- ABAQUS (1990). "User Manual, Version 5.3" Hibbitt, Karlsson, and Sorensen Inc. 1080 Main Street, Pawtucket, RI.
- Argyris, J. H. (1970) Matrix analysis of three-dimensional elastic media small and large displacements. American Institute of Aeronautics and Astronautics Journal, 3:45-51.
- Barron, R. A. (1948) Consolidation of fine-grained soils by drain wells. Trans. ASCE 113: 113-120.
- Bergado, D. T., Asakami, H., Alfaro, C., and Balasubramaniam, A.S. (1991) Smear effects of vertical drains on soft Bangkok clay, J. of Geotechnical Eng., ASCE, 117 (10):1507-1530.
- Carter, J.P., Booker, J. R., and Davis, E. H. (1977) Finite deformation of an elasto-plastic soil. International Journal for Numerical and Analytical Methods in Geomechanics. 1:25-43.
- Gale, S.M. (1998) Geotechnical review of embankment construction through 1997. Report No. 8, Proj. 95051, Gale-Tec Engineering, Minnetonka, MN
- Gale, S.M. (1999) Final geotechnical review of embankment construction. Report No. 15, Proj. 95051, Gale-Tec Engineering, Minnetonka, MN
- Lambe, T. W. (1973) Predictions in soil engineering. Geotechnique, 23:149
- Hansbo, S. (1987) Design aspects of vertical drains and lime column installation. Proc. 9th Southeast Asia Geotechnical Conf. , Bangkok, 8-1-8-12.
- Richart, F E. Jr. (1957) A review of the theories for sand drains. J. Soil Mechanics and Foundations Div., ASCE, 83 (SM3):1301-1 to 1301-38.
- Schiffman, R.L. (1958) Consolidation of soil under time-dependent loading and varying permeability. Proc. 37th Annual Meeting, Highway Research Board, 584-614.
- Schwepe, F.C. (1973) Uncertain Dynamic Systems. Prentis-Hall, Englewood Cliffs, NJ.
- State of Ohio (1996) FRA-670-1.14(A-1E), Columbus, OH.
- STS Consultants (1987) Geotechnical evaluation of embankment construction over softening sludge and landfill areas in conjunction with project FRA-670-1.25(A-1E) in Columbus, OH, STS Consultants, Minneapolis MN.
- STS Consultants (1993) Evaluation of sludge lagoon test section, Project FRA-670/315-1.25/0/00. STS Consultants, Minneapolis, MN.
- STS Consultants (1994) Geotechnical engineering associated with the I670 extension, Project FRA-670-1.14 (A-1E), STS Report 14, STS Consultants, Minneapolis, MN.
- Terzaghi, K. (1943) Theoretical Soil Mechanics. John Wiley and Sons, New York.
- Wu, T. H. (1996) Performance of a reinforced-soil embankment. Final Report, The Ohio State Univ., Columbus, OH.
- Zhou, S. X. (1995) Application of system identification to an embankment on sludge. Ph. D. dissertation, Ohio State University, Columbus, OH.